

DISSERTATION

EFFECT OF INTERPASS TEMPERATURE ON THE STRUCTURE AND  
PROPERTIES OF MULTIPASS WELDMENTS IN HIGH PERFORMANCE NICKEL  
ALLOYS

Submitted by

John S. Petro

Department of Mechanical Engineering

In partial fulfillment of the requirements

For the Degree of Doctor of Philosophy

Colorado State University

Fort Collins, Colorado

Summer 2011

Doctoral Committee:

Advisor: Frederick W. Smith

Walajabad S. Sampath

Susan P. James

Paul C. DuChateau

Dwaine Klarstrom

Copyright by John S. Petro 2011

All Rights Reserved

## ABSTRACT

### EFFECT OF INTERPASS TEMPERATURE ON THE STRUCTURE AND PROPERTIES OF MULTIPASS WELDMENTS IN HIGH PERFORMANCE NICKEL ALLOYS

Nickel alloys comprise an important group of engineering materials which are used primarily for their exceptional resistance to corrosion and their ability to maintain good mechanical strength over a wide temperature range, (both low and high) in demanding industrial applications. Welding is a primary fabrication process for these alloys. It has been a generally accepted practice to maintain a maximum interpass temperature of 200°F or lower when multipass welding many nickel alloys to prevent defects such as cracking or loss of corrosion resistance. This practice has been based on recommendations by many of the nickel alloy producers. A low maximum interpass temperature can increase the welding time which increases fabrication costs. According to the author's industry contacts and based upon the author's industrial experience as well as the author's examination of the literature, there has been little or no systematic research on the effect of interpass temperature for multipass welding of nickel alloys. In fact, the same is true for the establishment of the basic robotic welding parameters using the new generation of digital power supplies for these alloys.

This dissertation presents research on the effect of interpass temperature on two nickel alloys; HASTELLOY<sup>®</sup> C-2000<sup>®</sup> and HASTELLOY<sup>®</sup> B-3<sup>®</sup>. Welding parameters were also developed for these alloys and also for HAYNES<sup>®</sup> 230<sup>®</sup> alloy using Gas Metal Arc Welding, GMAW, as a single process for both the root and fill weld passes.

Weldments were made at 5 different interpass temperatures, 100°F - 500°F, in 100°F increments, for these alloys in thicknesses of 0.25 inch and 0.5 inch. Transverse weld specimens were then tested according to AWS B4.0:2007 using tensile, bend, and hardness tests. Transverse weld specimens were corrosion tested according to ASTM G28A for the HASTELLOY C-2000 alloy and the HASTELLOY B-3 alloy was subjected to 20% HCl at 149°C for 96 hours in an autoclave. The specimens were also examined using optical light microscopy for intergranular corrosion attack, weld fusion, cracking, and heat affected zone (HAZ) microstructure effects.

(HASTELLOY, HAYNES, C-2000, B-3, and 230 are registered trademarks of Haynes International, Inc.)

No significant loss of tensile strength was found at any of the higher interpass temperatures. All ultimate tensile strengths for both alloys were above the ASME Boiler and Pressure Vessel Code Section IX minimum. All samples passed 2T transverse face bend tests. Some lack of fusion was observed at the root of some samples at random interpass temperatures. No noticeable change in the HAZ microstructure or cracking was observed at the highest interpass temperature for both the HASTELLOY C-2000 and the HASTELLOY B-3 alloys.

No significant corrosion attack was found along the weld, face or root sides, for both alloys at the higher interpass temperature of 500°F.

It was concluded that a higher interpass temperature could be specified for these alloys without any appreciable loss of strength, weld soundness, loss of corrosion resistance, or detrimental effect to microstructure. It was also shown that the GMAW process could be used as a sole welding process but more development is needed to decrease process variability in the root pass and to develop a complete welding procedure specification.

## ACKNOWLEDGMENTS

The Author wishes to thank and express his sincere appreciation to all who have helped and lent assistance in this quest, especially:

Dr. Fred W. Smith, my advisor and Dr. Walajabad S. Sampath for their patience, understanding and guidance over 10 years.

Dr. Susan P. James and Dr. Paul C. DuChateau for making my CSU experience so meaningful.

Dr. Dwaine Klarstrom, Steve Matthews, Mark Britton, Mark Richeson, and everyone at Haynes International, Inc for their help, generous support and providing this research opportunity.

Doug Watkins, Kevin Summers, and the AMS Department at Miller Electric for their help and generous support.

Tony Daniel, my faithful assistant for his valuable help in machining and specimen preparation.

My brother Jeff, for his help with the impossible.

DEDICATION

*This dissertation is dedicated to*

*My wife, Jenny*

*and our children, John III, Shannon, Amanda, and Sean*

*whose love, support, understanding and encouragement*

*made this possible.*

*It is also dedicated to*

*my mother, Patricia*

*and to the memory of my father, John Sr.*

## TABLE OF CONTENTS

Chapter 1 Background .....	1
Chapter 2 Materials and Technical Approach .....	16
Chapter 3 Results and Discussion .....	39
Chapter 4 Conclusions .....	74
Chapter 5 Study Limitations .....	76
Chapter 6 Recommendations for Future Research .....	77
References .....	78
Appendix A Heating Fixture Drawing .....	82
Appendix B Temperature Controller Electrical Schematic .....	84

## **Chapter 1 Background**

### *Nickel Alloys*

Nickel alloys comprise an important group of engineering materials which are used primarily for their exceptional resistance to corrosion and their ability to maintain good mechanical strength over a wide temperature range, (both low and high) in demanding industrial applications. The element Nickel is a metal in group 10 on the periodic table. Nickel has a face-centered-cubic (FCC) crystal structure which is one of the reasons it has good formability [1, 2]. In 1990, approximately 13% of the nickel produced went into making nickel based alloys, 57% into stainless steels and much of the balance into other alloy and plating applications [1]. Nickel has extensive solid solution solubility with many other elements. Because of this, nickel can be alloyed with elements such as copper, chrome, iron, molybdenum, tungsten, tantalum and others to form various specialty alloys with good corrosion and heat resistance properties [1, 3]. Nickel may be strengthened by solid-solution hardening, carbide strengthening, and precipitation hardening [1]. Nickel alloys are expensive and therefore are only used in those critical or demanding applications requiring the optimal performance in corrosion and/or high temperature environments. Industries and applications using nickel alloys include: gas

and steam turbines, tools and dies in metal processing, rocket engine parts, pollution control equipment, chemical and petrochemical processing, heat treating equipment, and in paper and pulp mills. Many of these applications require welding as the primary joining process.

## *Applications*

### **Nuclear Waste Containers**

The recent record prices for oil have renewed the debate over alternative energy sources. Nuclear power plants are one of the alternatives in this renewed discussion. One of the contentious issues of nuclear power is the disposal of high level nuclear waste. Nickel alloys are being investigated as a possible material for the outer shell of a container for the safe disposal of high level nuclear waste. The containers would be stored in deep underground, geological repositories. The current time requirements for which the container must remain intact range from 10,000 to 1,000,000 years [4]. One of the many complicating factors for containment is the heat generated by the radioactive decay of the waste. The temperatures that a container might experience could be as high as 320°F (160°C) for the first 1,000-1,800 years of storage [5, 6]. The devastating March 11, 2011, earthquake, (9.0 on the Richter scale), and resultant tsunami in Japan reinforce the need for safe storage and containment of nuclear materials in reactors and as spent fuel.

### **Ultrasupercritical Boiler Applications**

The need for economical and abundant electrical power for the growing world presents a big political and engineering challenge. The reserves of world oil seem uncertain but many countries have enormous coal reserves. These reserves could provide the energy for much of the future demand of electricity through coal-fired steam generation plants. In steam generation, increased thermodynamic efficiency can be obtained by operating at higher steam temperatures and pressures. The increased efficiency will come with steam conditions in the ultrasupercritical range of 1,400°F (760°C) and 5,000 psi, ultrasupercritical steam conditions (USC) [7]. These conditions present many material

challenges for oxidation and fireside corrosion resistance, creep as well as for fabrication and stress considerations. Nickel alloys have some great advantages in these applications [8, 9].

### **Aero and Land Based Gas Turbine Engines**

Gas turbine engines present similar engineering material problems because of the high temperature and corrosion environment they operate in. As the turbine industries continually improve designs and efficiencies, a higher demand is put on the materials used in construction. Nickel alloys provide the fatigue strength, long term thermal stability, and reparability for many of the components in gas turbine engines [10, 11, 40].

### ***Fabrication***

The applications cited above as do many others require welding as a primary fabrication process. Weldability, how easily a material can be welded, is an important consideration in alloy selection. In the case of critical applications such as boilers and pressure vessels; the materials, construction and welding is governed by welding codes and standards. Two widely recognized codes are the ASME Boiler and Pressure Vessel Code [12, 45] and the ANSI/AWS Structural Welding Code D1.X (X denoting the material or end use).

Welded construction of the tanks, columns, chemical reactions vessels, and many other components require complete joint penetration by the weld. For many of these types of weldments, this requires a type of weld joint known as a groove weld, Figure 1.

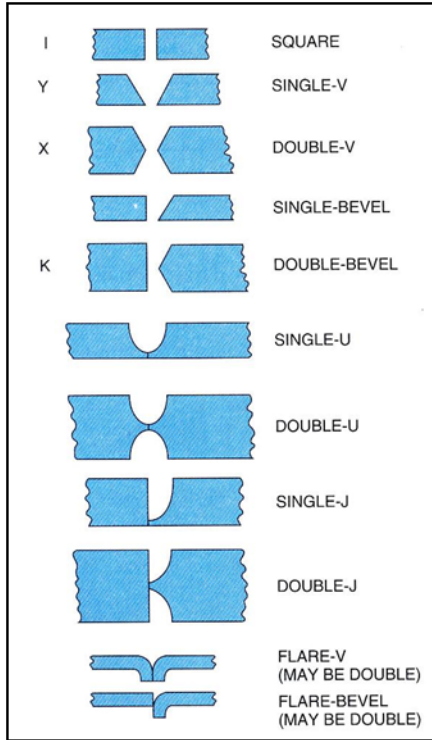


*Figure 1 Groove Weld Types*

Groove welds are classified into different types based on the geometry of the weld cross section, such as square, V-, bevel, U- and J-. The groove weld allows welding access to the entire material thickness and this allows any loads to be effectively transferred across the weld joint, thus maintaining the base material's cross sectional mechanical properties. Groove welds generally require multiple weld passes to fill the weld joint.

### **Weld Zone**

The heat input of the welding arc melts the base metal and filler metal. The accompanying thermal gradients cause distinct metallurgical areas to form in and along the weld joint. In a single pass weld these areas can be simplified as: 1.) The Weld – the melted base metal and filler metal, 2.) The Heat Affected Zone (HAZ) – the portion of

the base metal that has not melted but where the temperature was raised high enough to change the material microstructure and mechanical properties, and 3.) The Unaffected Base Metal [13], as shown in Figure 2.

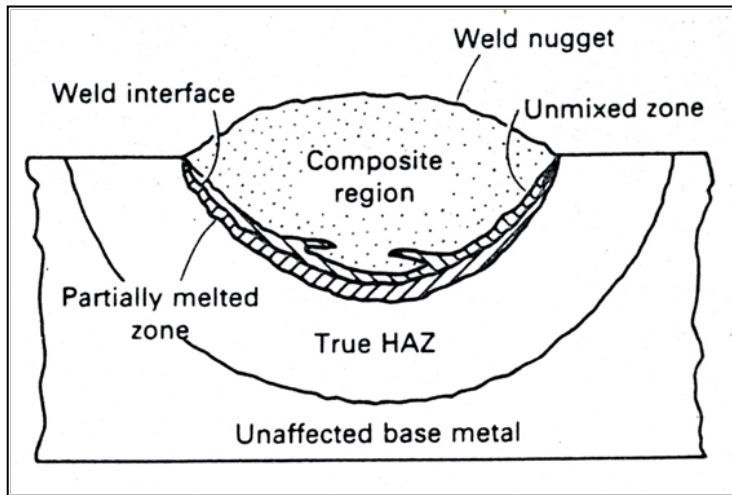


*Figure 2 Metallurgical Zones of the Weld. Source: Ref 48*

In a multipass weld, the situation is further complicated by the thermal gradients caused by the subsequent weld passes on the microstructures of the previous weld beads. The microstructural changes of the underlying weld beads depend on the welding process and parameters used (thermal cycles). Depending on the base material's composition, special welding procedures may be needed to maintain the integrity of the weld and surrounding area to prevent various defects from occurring such as cracking from a microstructure that has become too hard and brittle[14]. These procedures usually are in the form of a preheat or a post heat of the weldment to prevent or control some microstructural transformation. In multiple pass welding one of these procedures is to control the interpass temperature.

### ***Interpass Temperature***

Interpass temperature is defined by the American Welding Society in the following way:

*“In a multipass weld, the temperature of the weld area between weld passes”* [15].

Although this description is general in nature, it is of extreme importance in welding that is covered by codes such as the ANSI/AWS Structural Welding Code for Steel [16] and the ASME Boiler and Pressure Vessel Code. When welding ferrous alloys, a controlled interpass temperature slows the cooling rate through an alloy's critical temperature to prevent defects from happening during multipass welding [17]. A Preheat temperature is the equivalent of interpass temperature but for a single pass weld. The interpass temperature can be specified as either a minimum or a maximum temperature depending on the material being welded. A minimum interpass temperature is specified for many ferrous alloys. This minimum temperature is used to prevent the weld from cooling too rapidly and causing the microstructure to transform from austenite to martensite which could result in weld cracking because of rapid volume change and shrinkage [14, 18]. The effect of interpass temperature on steels and ferrous based alloys has been well studied and continues to be researched for new alloys and processes using physical experiments or numerical models [19-27].

### ***Maximum Interpass Temperature***

In the case of welding nickel alloys, a maximum interpass temperature is specified.

Corrosion resisting nickel alloys for example contain large amounts of alloying elements to give this property. At high temperatures many alloying elements are easily dissolved in the nickel matrix and then when cooled to room temperature during manufacture these alloying elements remain in solid solution and a single phase FCC microstructure.

However if these nickel based alloys are exposed after manufacture to high temperatures above 930°F (500°C) for different periods of time, deleterious second phase precipitates may form that can change mechanical and corrosion properties in the HAZ [6].

The intent of a maximum interpass temperature is to prevent undesirable carbide or intermetallic phases from precipitating in the HAZ. As a general statement, higher heat input into the weldment will tend to expose more material to higher temperatures, longer, where undesirable reactions such as secondary carbide precipitation, grain growth, and grain boundary liquation can occur in the HAZ, leading to cracking, loss of corrosion resistance, and reduced mechanical properties [6, 28]. This is true for both corrosion resistant nickel alloys and heat resistant nickel alloys. Some of these carbides, generally labeled  $M_xC_x$ , where M stands for the metallic carbide forming element(s), such as molybdenum, Mo, chromium, Cr, tungsten, W, for example, and C standing for carbon, can form in the grain structure or along grain boundaries and impair ductility, creep rupture life, and corrosion resistance [1]. The terminology “grain boundary liquation” refers to phases or particles that have precipitated along the grain boundary and melt below the bulk material melting temperature [29]. This can cause weld metal solidification cracking (also called hot cracking) and microfissuring. As the molten weld pool starts to solidify, the liquid weld metal starts to contract because of thermal contraction and solidification shrinkage. This tends to put the weld in a state of tension as the bulk base metal also contracts but not as much since it has not melted or become as hot. Low-melting-point films develop along the solidification grain boundaries as some of the alloying elements segregate there. The strain that develops upon weld solidification causes separation along the grain boundaries which lead to a crack [30-31].

Weld metal microfissuring is similar to solidification cracking but is sometimes defined as cracks appearing in the weld bead below the subsequent weld pass.

Another problem which can occur is sensitization, when material in the HAZ is exposed to higher temperatures and longer times, chromium combines with other carbides that precipitate out at the grain boundaries leaving the surrounding area depleted of corrosion resisting elements [1]. The depleted area becomes anodic compared to the rest of the grain which leads to intergranular corrosion attack (IGA) similar to the problem in stainless steels.

The above are all reasons why interpass temperatures were recommended to be as low as possible. In this research project, many of the defects described above can potentially come from two general areas. The first being the welding process itself. This would include defects such as lack of fusion, cracking, porosity and the like. These are a function of using the correct welding variables such as voltage, amperage, filler material, shielding gas, gas flow rate, travel speed, weld position, etc. The other area of concern is the intended service conditions for the weldment. The focus of the research project is to answer the question how does the interpass temperature affect the weldment's ability to perform under the intended service conditions such as corrosion resistance and its affect on other mechanical properties. The purpose of this research project is to quantify that interpass temperature effect. In conducting this research, it also became necessary to identify certain basic welding parameters for these materials since such information was also found to be unavailable in the literature for the newer generation of digital welding power supplies.

### ***Literature Review***

The author has not found any published studies about the effect of interpass temperature on high performance nickel alloys other than manufacturer's recommendations and such recommendations are based on anecdotal experience [32, 33] and (Steve Matthews, Haynes International, Inc., Personal Correspondence, February 04, 2008). Weldability studies for these alloys have been published but the interpass temperature was always maintained at 200°F (93°C) and never separately studied as a welding parameter variable [11, 30, 31, 34, 35, 36,44].

Research studies involving several ferrous alloys are discussed below.

Ginn *et al.* [27] tested several austenitic stainless steels (304L, 316L, & 316H) and welding processes with interpass temperatures ranging from 100-400°C (212-752°F).

Their results indicated that higher interpass temperatures could be used with these alloys and that the higher temperatures had no effect on mechanical properties and weld microstructure.

Omar [26] did an experimental study of dissimilar metal welds in carbon steel – austenitic stainless steel transition joints with electrode composition and preheat/interpass temperature as variables. This study found that interpass temperature and electrode composition did have an effect on hard zone formations in the weld joint. This research recommended an optimum preheat and interpass temperature along with electrode composition for the materials and weld joint of the study.

Lee [22] also studied several welding variables related to austenitic stainless steel including interpass temperature. His findings indicated that increased preheat and

interpass temperature increased the degree of sensitization and the width of the sensitized zone.

Beres [19] did not perform any experiments with interpass temperature but proposed a new idea in calculating an optimized interpass temperature for air hardening steels.

## **Problem Statement**

The purpose of this research is to determine robotic welding parameters for HASTELLOY<sup>®</sup> C-2000<sup>®</sup>, HASTELLOY<sup>®</sup> B-3<sup>®</sup>, and HAYNES<sup>®</sup> 230<sup>®</sup> using modern, software based, digital welding power supplies and the effect of interpass temperature on the microstructure, mechanical properties, and corrosion resistance of multipass weldments in high performance nickel alloys. A secondary purpose of this research is also to investigate the feasibility of using the same welding process for the root pass as is used for the fill passes. This is of interest because current practice and some welding codes [12, 45] specify the GTAW process for the root pass and it would be much easier and save time if one process, GMAW for example, could be used for the root pass and all of the fill passes of a multipass weldment.

## ***Benefits of Understanding Interpass Temperature***

Much of what is currently known about the multipass welding of high performance nickel alloys comes from the manufacturer or is from the practical experience of the fabricators rather than from systematic research. Welded components from nickel alloys comprise a wide range of critical applications as discussed earlier so any new process information is important. Practical benefits from being able to use increased maximum interpass temperatures include:

*(HASTELLOY, HAYNES, C-2000, B-3, and 230 are registered trademarks of Haynes International, Inc.)*

- 1.) Increased productivity, less wait time between weld passes for the weldment to cool down.
- 2.) In applications where nickel alloys are used as a weld overlay cladding on steels, better fusion and less chance of welding defects. (The steel temperature must be kept above the martensite start temperature)
- 3.) The use of nickel alloys in unusual applications such as the high level nuclear waste containers where the nuclear waste temperature is already above 200°F (93°C).

### ***Benefits of Using a Single Welding Process in Multipass Welding***

In the complete penetration joints for nickel alloys, the root pass is generally put in using Gas Tungsten Arc Welding (GTAW) because of the process's high quality. The GTAW process uses a nonconsumable electrode of tungsten to maintain the welding arc to the base metal while an inert gas provides shielding to the molten weld pool from contamination of the atmosphere, Figure 3. GTAW is superior to GMAW, because it allows for precise independent control of the heat input and filler metal for consistent results. The GMAW process, Figure 4, instead uses the filler metal as a consumable electrode and is not able to provide the same level of precise independent control. Using the GTAW process for the root pass is also a welding code requirement for the welding fabrication of many pressure vessel applications. This quality does come at a cost though; GTAW is a high skill process, generally has slower travel speeds, and lower weld deposition rates. A trend in welding fabrication for economy is to try and eliminate these different processes and use only one process where possible [40]. Doing this simplifies

the welding procedure and reduces the cost of fabrication. This can be possible because of the advancements in software based welding inverter power supply technology.

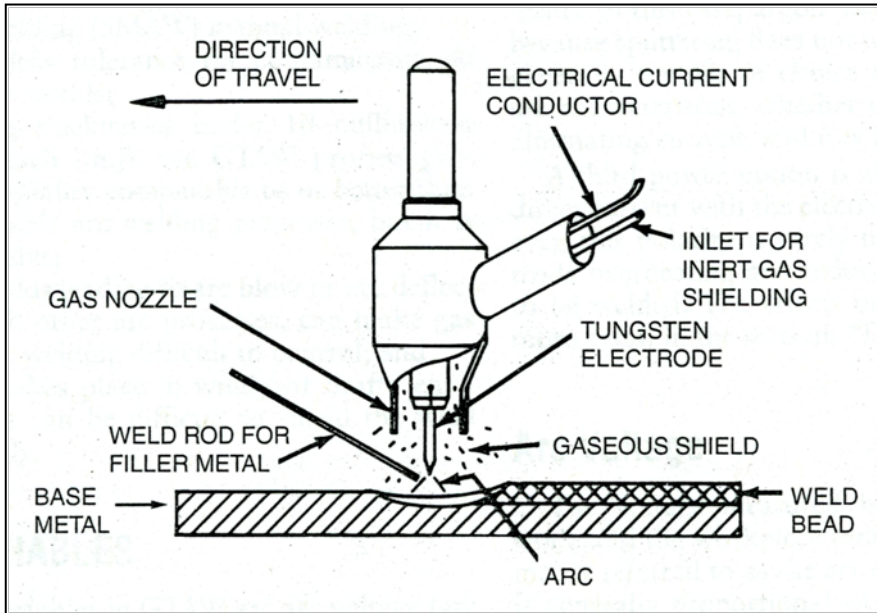


*Figure 3 GTAW Process (Manual). Source: Ref 49*

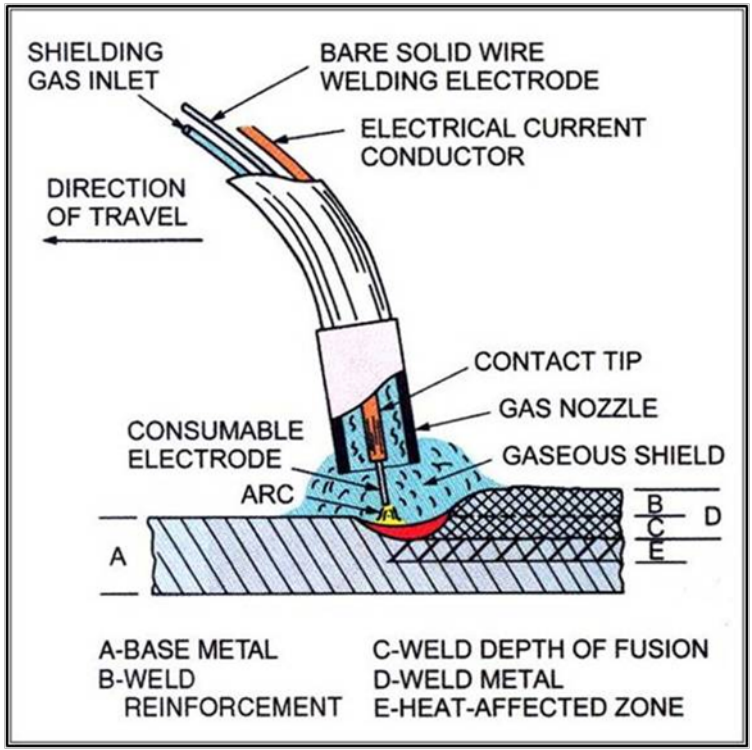


Figure 4 GMAW Process. Source: Ref 49

## Chapter 2 Materials and Technical Approach

### *Nickel Alloys Used In This Research*

The nickel alloys used in this research were provided by Haynes International, Inc., Kokomo, Indiana. These alloys were chosen because they are commercially important and are used widely in industrial applications. The two corrosion resistant alloys represent opposite ends of corrosion resistance applications; the C- family which is based on the Ni-Cr-Mo system and the B- family which is based on the Ni-Mo system. The heat-resistant alloy was chosen as a comparison to the corrosion resistant alloys. The following paragraphs discuss these materials.

### **Solid Solution Strengthened Corrosion-Resistant Alloys**

#### ***HASTELLOY C-2000 Alloy (UNS N06200)***

This is a versatile corrosion resistant alloy designed for the chemical processing, pollution control, and other industries to resist acids over a wide temperature range. This alloy is based on nickel, chromium, and molybdenum and has excellent corrosion resistance in both oxidizing and reducing acids.

Nominal Chemical Composition, wt.% [37]

<b>Ni</b>	<b>Cr</b>	<b>Mo</b>	<b>Fe</b>	<b>Cu</b>	<b>Al</b>	<b>Mn</b>	<b>Si</b>	<b>C</b>
59(bal)	23	16	3*	1.6	0.5*	0.5*	0.08*	0.01*

\*Maximum

***HASTELLOY B-3 Alloy (UNS N10675)***

This is a nickel-molybdenum family of alloys with excellent resistance to hydrochloric acid. B-3<sup>®</sup> has a high level of thermal stability. Thermo stability is a material's ability to maintain ductility through thermal cycles that might be experienced during fabrication.

Nominal Chemical Composition, wt.% [38]

<b>Ni</b>	<b>Mo</b>	<b>Cr</b>	<b>Fe</b>	<b>Co</b>	<b>W</b>	<b>Mn</b>	<b>Al</b>	<b>Ti</b>	<b>Si</b>	<b>C</b>
65(min)	28.5	1.5	1.5	3*	3*	3*	0.5*	0.2*	0.1*	0.01*

\*Maximum

**Solid Solution Strengthened Heat-Resistant Alloy**

***HAYNES 230 Alloy (UNS N06230)***

This is a nickel-chromium-tungsten-molybdenum alloy designed for high-temperature gas turbine engine components and also finds use in the chemical processing and industrial heating industries. This alloy displays a good combination of high temperature strength and corrosion resistance as well as weldability.

Nominal Chemical Composition, wt% [39]

<b>Ni</b>	<b>Cr</b>	<b>W</b>	<b>Mo</b>	<b>Fe</b>	<b>Co</b>	<b>Mn</b>	<b>Si</b>	<b>Al</b>	<b>C</b>	<b>La</b>	<b>B</b>
57(bal)	22	14	2	3*	5*	0.5	0.4	0.3	0.10	0.02	0.0015*

\*Maximum

### *General Experiment Overview*

All the alloys used in this study came from single individual heats of materials for consistency. The material was supplied in the form of wrought alloy plate in the solution heat-treated condition. This research project consisted of robotically welding the three nickel alloys discussed above, Figure 5, at various interpass temperatures.

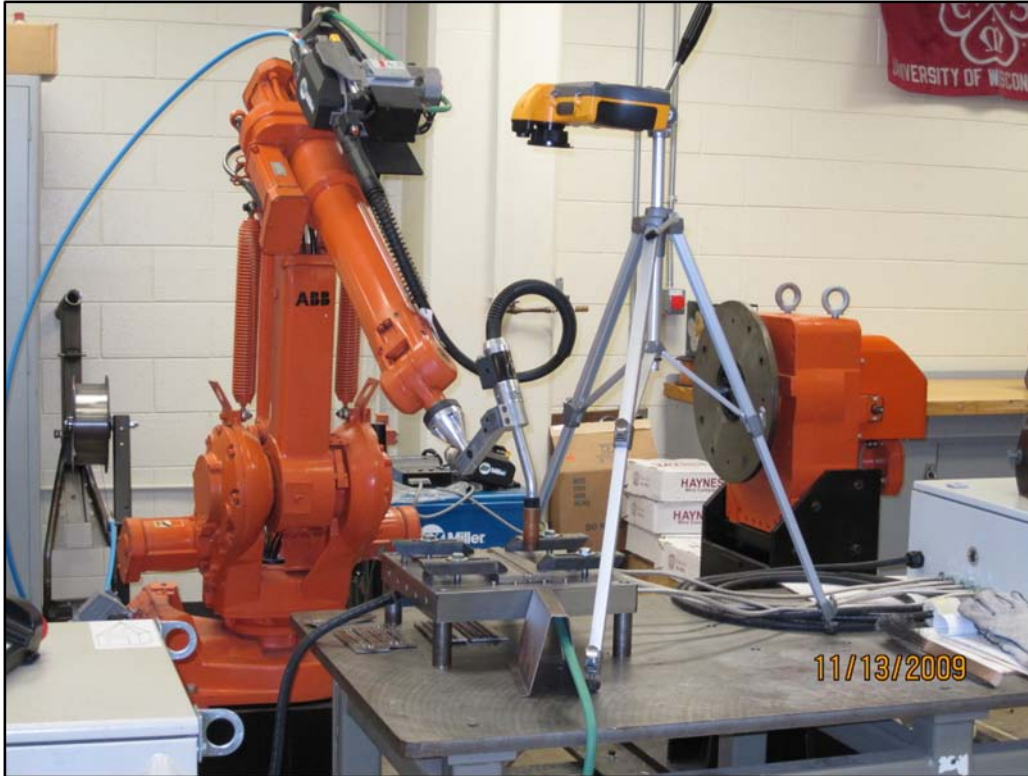


*Figure 5 Experiment Set Up*

The GMAW, (Gas Metal Arc Welding), process was used for all welds, (root and fill passes). Two thicknesses of each alloy were welded at five interpass temperatures and tested according to the Table 1 below.

**Table 1 Experiment Overview**

<b>Alloy</b>	<b>Weldment Thickness (Inch)</b>	<b>Interpass Temperature °F</b>	<b>Tests (C-2000 &amp; B-3 only)</b>
<i>HASTELLOY C-2000</i>	0.25 (6mm) 0.50 (12.7mm)	100 (38°C) 200 (93°C) 300 (149°C) 400 (204°C) 500 (260°C)	Transverse Tensile Transverse Guided Bend: Face, Root, Side Optical Microscopy Corrosion Hardness
<i>HASTELLOY B-3</i>			
<i>HAYNES 230 Alloy</i>			

Two weldments were made at each test condition for a total of 60 weldments, 20 for each material type. The weldments were rigidly clamped in a fixture with variable heating elements to control the interpass temperature. The interpass temperature was monitored using a hand held thermocouple probe calibrated to a known standard probe. A thermal imaging camera was also used. After the final welding pass, the weldment was removed from the fixture and allowed to cool in still air to ambient temperature. The completed weldments of alloys C-2000 and B-3 were then sectioned for mechanical, metallurgical, and corrosion testing.

### ***Welding Consumables***

Listed in Table 2 below are the filler materials used for welding study. The filler material is of the same composition as the base material for maintaining corrosion resistance and weldability.

**Table 2 Welding Consumables**

<b>Material</b>	<b>Welding Filler Wire -0.045" Dia.</b>
HASTELLOY C-2000	ER-NiCrMo-17
HASTELLOY B-3	ER-NiMo-10
HAYNES 230 Alloy	ER-NiCrWMo-1

### ***Weldment Preparation***

The as-received material in plate form, in the solution heat-treated condition, was sawed and sheared into 10 inch lengths. The individual 10 inch sections were then machined with a 35 degree bevel angle and a root land. The dimensions of the root land and opening would be determined from the development of the welding parameters. This was done to produce a single groove weld joint that would be consistent and repeatable for robotic welding, Figure 6.

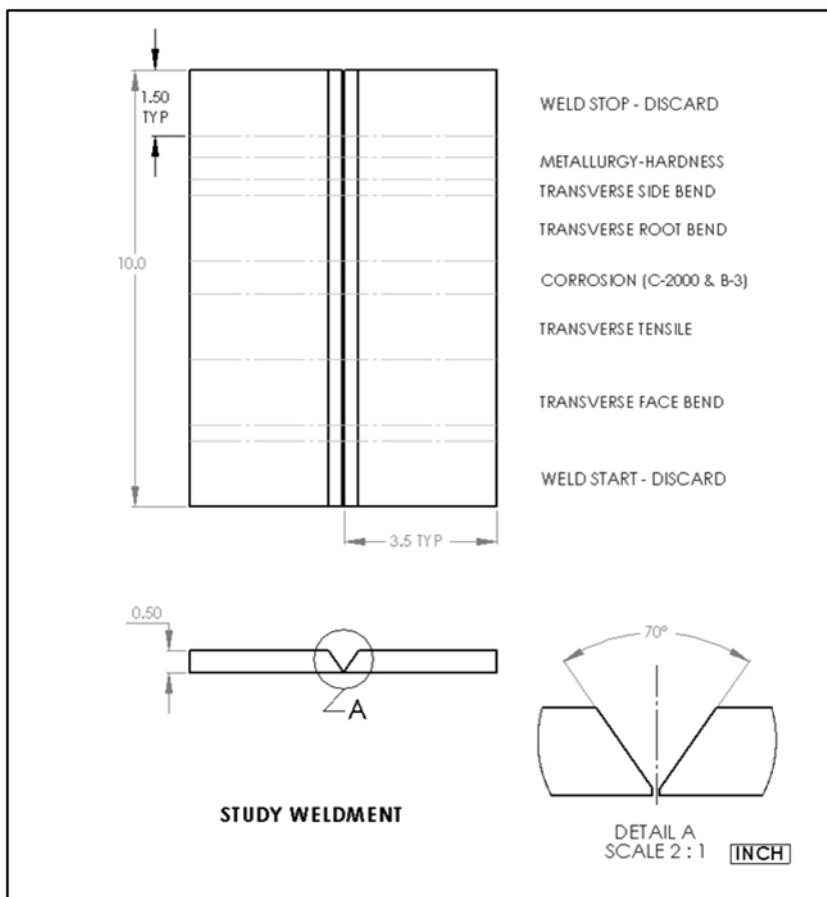


***Figure 6 Study Weldment***

The top and bottom plate surfaces were also ground with an 80 grit flap wheel to remove any mill scale and for a consistent finish between all weldments.

### ***Welding/Heating Fixture***

The welding/heating fixture, Figure 7, was made from a 2 inch x 14 inch x 14 inch, AISI/SAE 1020 Hot Rolled Steel, HRS, plate that was ground top and bottom with all sides machined square and parallel. The fixture plate was machined to receive 5 Watlow 1000 watt heating cartridges spaced evenly through the center. The rods were installed to the manufacture's recommended hole diameter tolerances for optimum heat transfer between the rods and fixture plate. The heating rods were connected to a PID programmable temperature controller with a feedback thermocouple that was mounted in the center of the fixture. A 0.125 inch wide channel was also machined in the fixture's top surface to provide a back-purge shielding gas path for welding of the root pass. 6 strap clamps, 3 per weldment side with 0.5 inch – 13, Unified National Course, UNC, grade 8, Hex Head Cap Screws, HHCS, secured the weldment during welding.

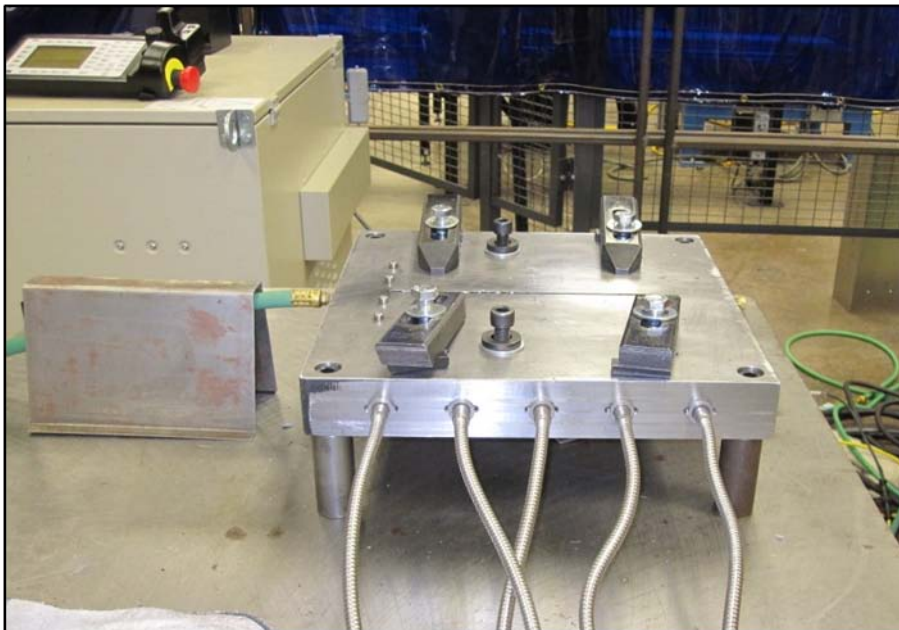


***Figure 7 Welding/Heating Fixture Unloaded***

This type of clamping provided a highly restrained condition for the weldment. This type of restraint would be similar to fabrication conditions and also tend to show any evidence of solidification cracking during welding. The fixture was supported on 2 inch diameter x 3 inch high risers at the four corners to minimize heat loss to the welding table.

### ***Robot and Welding System***

An ABB IRB1400 robot with a Binzel welding torch mounted on the end of robot axis 6 was used to provide consistent and repeatable weld passes for the study. This allowed for uniform travel speeds and weld angles. The welding power supply used was a Miller Electric Auto- Access 450, a new generation of digital welding power sources. These digital power supplies use faster, more powerful micro processors that can receive feedback from the welding process and optimize the welding waveform for all phases of the welding process. This allows for continual optimization of the arc to account for condition changes during welding and also allows the welding wave form to be fine tuned to the material and joint geometry. The welding robot and Miller Electric power supply are shown in Figure 8.

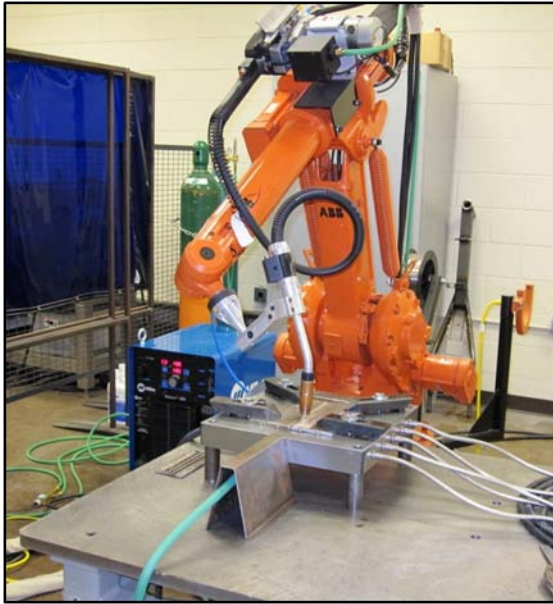


***Figure 8 Robot and Power Supply***

## ***Welding Procedure***

### **Root Pass**

All root passes were performed at room temperature and in the flat position, (AWS 1G). This would be consistent with field conditions where the weldment would be at room temperature for the start of the multipass welding sequence. The root pass is important as this sets the joining foundation for all the welds that come after. If the root pass is not done correctly, a welding defect will surely originate from here. One of the most common defects is incomplete fusion where one or both sides of the joint are not metallurgically joined (melted together). The root pass used the Miller Electric Co., RMD™, (regulated metal deposition) process. This process is a modified GMAW short circuiting deposition that digitally controls short circuit transfer to reduce weld spatter and heat input into the weldment.

### **Fill Passes**

The fill passes were welded in the flat position, (AWS 1G). All fill passes were put in as stringer beads (no side-to-side weaving motion) to reduce heat input from welding. The weldment was clamped to the weld fixture and the weld fixture was then brought to the desired interpass temperature. After each fill pass, the completed weld and surrounding area were wire brushed to remove any weld spatter or oxidation before the next pass was started. A GMAW pulsed spray transfer welding process was used for all fill passes. The fill pass process used was a Miller hybrid GMAW process called Accu-curve™ which is a variation of the Accupulse™ process. The Accu-curve™ process uses a 2<sup>nd</sup> degree curve to transition between background to peak and peak to background current levels instead of a linear transition. This can give smoother welding transitions between

amperage levels. The new processes use digital software based welding waveform control for the improved performance.

### *Temperature Measurement*

#### **Handheld Thermocouple Surface Probe**

The temperature of the weldment surface was measured using a hand held Fluke 80PK-27 surface temperature probe connected to a Fluke series 52 thermometer, Figure 9.



*Figure 9 Fluke Thermometer and Probe*

Temperature readings were taken before and after the welding of each fill pass at 6 locations approximately 0.5 inches on either side of the weld centerline, 3 per side, on the top surface. The surface readings were generally within 1-2 °F at the measurement locations for the lower interpass temperatures (100-300 °F) and within 5-6°F for the

higher interpass temperatures, (400 & 500 °F). The temperature measuring sequence was as follows:

1. Bring the weld fixture and weldment up to the desired interpass temperature and stabilize, approximately 60 minutes.
2. Weld
3. Measure the weld surface and either side of weld centerline until the temperature falls back to the interpass temperature.
4. Weld the next fill pass.
5. Repeat steps 3 and 4 until the weld joint is filled.
6. Remove the completed weldment from the fixture and allow to cool in still air.

This procedure and equipment would be one way the interpass temperature would be monitored in the field by fabricators and why it was chosen.

### **Thermal Imaging Camera**

A Fluke Ti45FT IR thermal imaging camera was also used in the study as a non contact method to accurately determine surface temperature. The thermo couple surface probe, thermo imaging camera, and the temperature controller's thermo couple were originally combined to serve as checks on each other that the interpass temperature desired was actually being accomplished. This was not the case. Several obstacles prevented this from happening. The first being the determination of an emissivity constant for the material. Thermal imaging equipment requires that an emissivity constant,  $\epsilon$ , be determined for the material to measure its surface temperature. Emissivity is a measure the thermal energy that is being emitted from a material. The  $\epsilon$  value is a ratio of the thermal energy from a perfect emitter, known as a black body, to the amount of thermal

energy being emitted from the material in question. The emissivity value is a number between 0 and 1. Generally the  $\epsilon$  value is different for every material and the material's surface finish as well. There are several techniques to determine a material's  $\epsilon$  value. One method uses the temperature reading from another temperature reading instrument, such as a thermocouple surface probe or thermometer, to measure the surface temperature and then use this value to calibrate the material's  $\epsilon$  value to the thermal imaging camera. Some of the other methods were not practical to this welding study or were too costly to use. A second obstacle from determining an emissivity constant was for many metals, nickel being one, the  $\epsilon$  value changes as the temperature changes. The exact surface temperature is difficult to obtain with a thermal imaging camera. All this being said, the thermal imaging camera was useful in providing a map of the relative temperature distribution on the weldment's surface, Figure 10. The thermocouple surface probe was relied upon to take the interpass temperature readings for the reasons stated above.

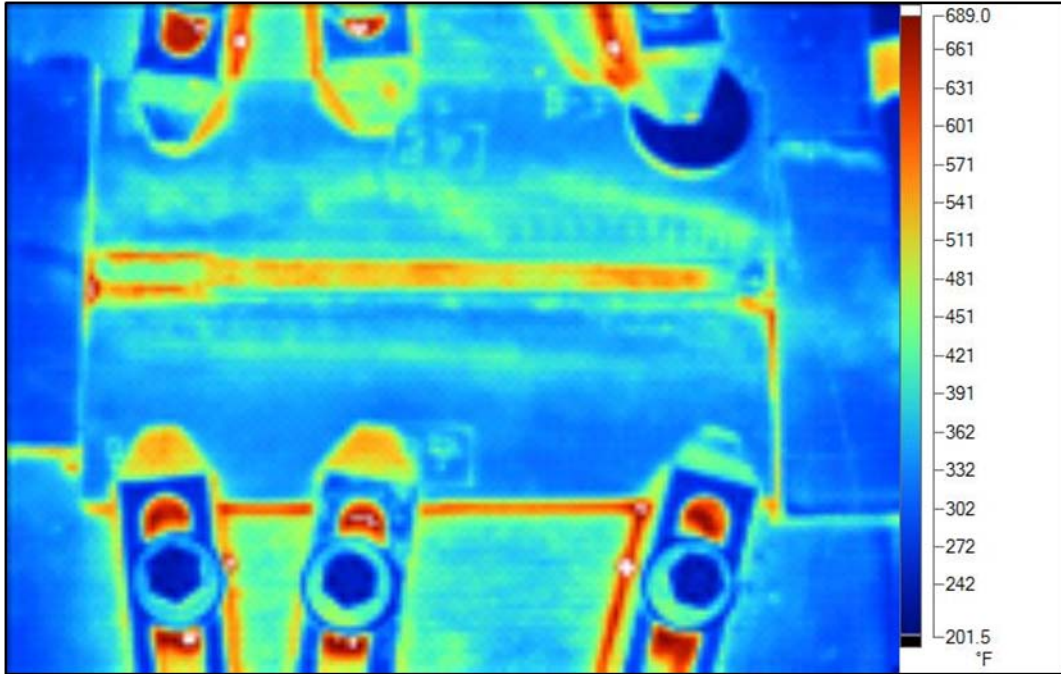


*Figure 10 Thermal Image of a B-3 Weldment*

### ***Weldment Sectioning***

The completed weldments were sectioned transversely across the weld for mechanical, corrosion and metallurgical testing specimens by water jet cutting, Figure 11. This process was chosen because of the low heat input into the weldment test pieces.

Additionally, the nickel based alloys are classified as moderate to difficult to machine by many conventional methods. Using the water jet process eliminated the cutting and machining issue. Although this is an expensive process, the benefits outweighed the cost in test sample preparation. Bend, tensile, corrosion, and metallurgical samples were cut to size with minimal heat and distortion.

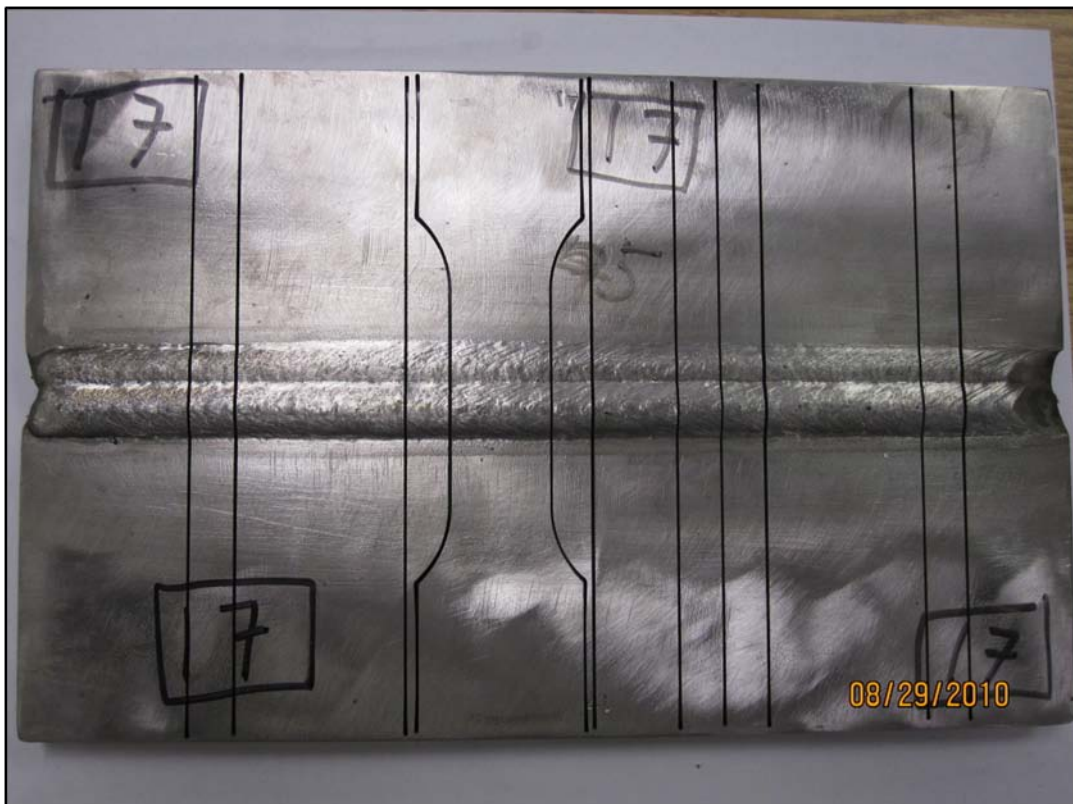


***Figure 11 Water Jet Sectioned Weldment***

## ***Testing***

### **Mechanical Testing**

The mechanical properties of the weldments were determined from tensile, guided bend, and Rockwell hardness testing. Transverse weld specimens were tensile bend, and hardness tested in accordance with ANSI/AWS B4.0:2007, Standard Methods for Mechanical Testing of Welds [41]. For this study only the corrosion resistant alloy weldments, C-2000 and B-3 were tested. The test samples for the HAYNES<sup>®</sup> 230<sup>®</sup> alloy weldments are prepared and will be tested in the fall of 2011 in a high temperature alloy study.

### **Tensile Test**

The tensile test specimens were sectioned transverse to the weld centerline with the center of the gage length centered on the weld. The tests were done on a Tinius Olsen 60,000 lb hydraulic universal testing machine, Figure 12.



*Figure 12 Tinius Olsen Universal Tester*

The strain rate was in accordance with ASTM Standard E8-04, Standard Testing Methods for Tension Testing of Metallic Materials [42]. The crosshead displacement rate was maintained at .125 inch/min to 5% strain rate and then increased to 0.5 inch/min until the completion of the test. All specimens with the exception of the 0.5 inch thick B-3 samples were tested at these rates. The B-3, 0.5 inch thick specimen was tested at 0.125 inch/min to 5% strain and then at 0.4 inch/min to test completion. The lowered test rate was used to preserve gripping jaw life. All test rates were within the ASTM E-8 standard. Only the Ultimate Tensile Strength was reported per the AWS B4 standard.

### **Transverse Weld Guided Bend Test**

Guided bend tests were done using a bottom type guided bend fixture, Figure 13. The plunger radius was twice the material thickness, (2T). The weld reinforcement on the root and face was removed according to ANSI/AWS Standard B4.0:2007. Figure 14 shows the test specimen locations in the weldment for the various bend orientations, face, root, and side.



*Figure 13 Bottom Type Guided Bend Fixture with Test Specimen*

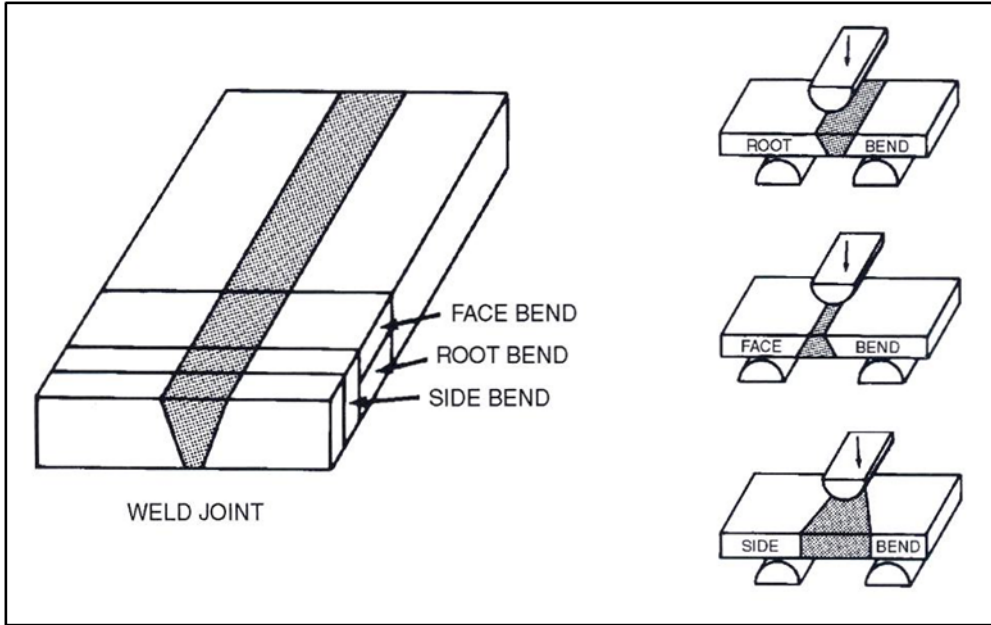


*Figure 14 Transverse Bend Test Specimen Locations. Source: Ref 50*

The bend specimens were tested in accordance with Table 3.

**Table 3 Transverse Weld Guided Bend Tests**

<b>Material</b>	<b>Plate Thickness inch (mm)</b>	<b>Plunger Radius inch (mm)</b>	<b>Bend Test per Weldment</b>
<b>HASTELLOY C-2000</b>	0.25 (6.4)	0.50 (12.7)	1 Face 1 Root
<b>HASTELLOY C-2000</b>	0.50 (12.7)	1.0 (25.4)	1 Face 1 Root 1 Side
<b>HASTELLOY B-3</b>	0.25 (6.4)	0.50 (12.7)	1 Face 1 Root
<b>HASTELLOY B-3</b>	0.50 (12.7)	1.0 (25.4)	1 Face 1 Root 1 Side

### **Hardness Testing**

Rockwell hardness tests on the B scale were made with a 0.062 inch diameter carbide ball indenter and a 100 Kgf load. Indentations were taken on the transverse sectioned specimens in the weld and in the adjacent base material.

### **Weldment Corrosion Testing**

Corrosion resistance is an important property for nickel based alloys. These alloys are used in extreme chemical environments in many processing industries, such as petrochemical, pharmaceutical and power generating. The thermal heating and cooling cycles of the welding process can cause localized changes in the microstructure, composition, and stress levels of the weld and adjacent base metal. These localized structure and composition changes can affect the material's corrosion resistance. Because of this, corrosion in nickel based weldments will many times start at or near the welds. During welding, carbides and intermetallic phases can solidify along grain boundaries and deplete the surrounding area of alloying elements that are essential to corrosion resistance. This is known as intergranular attack (IGA) or intergranular corrosion (IGC) [46]. There are many standardized tests used to evaluate a material's resistance to corrosion. The tests used in this research are listed below. The corrosion testing for this study was performed by Haynes International at their Kokomo, IN facility.

### ***HASTELLOY C-2000***

ASTM G28A/A262B, (Streicher Test) [43]

This test was used for the Hastelloy C-2000 alloys. The test consists of placing the specimen in a boiling solution of ferric sulfate-50% sulfuric acid for 24 hours. The specimen is weighed before and after the test. The result is reported as a corrosion rate in mils/year using a predefined formula. This rate can then be compared to a base rate for the alloy. Generally this corrosion rate has little meaning for weldments so a metallographic examination of the weld and HAZ area adjacent to the fusion line of the weld is done to evaluate intergranular corrosion attack, (IGA). The four corners of the fusion faces along the fusion line, top and bottom weld surfaces, are microscopically examined for any evidence of IGA and the maximum depth of corrosion attacked is reported.

### ***HASTELLOY B-3***

The test used for the Hastelloy B-3 alloy was not a test standardized by ASTM. It is from a British Petroleum corrosion test. In this test the specimen is immersed in 20% HCl at 149 °C for 96 hours in an autoclave. The specimen is weighed before and after. A corrosion rate is reported in mils/year as in the G28A test but as mentioned previously has little significance for weldments. The top and bottom fusion faces are also microscopically checked for any IGA and the maximum depth of attack is reported.

## **Metallography**

Transverse weld samples from the as received 0.5 inch thick plate before welding, 200°F and 500°F interpass temperatures were polished, chemically etched, and examined under a light optical microscope. These samples were chosen for general representation and as preliminary indicators of any significant microstructure variances. The samples were mounted in a clear epoxy resin and then ground with abrasive discs from 220 thru 600 grit. The samples were then polished with 9 and 3 $\mu$ m diamond suspension followed by a final polish with 0.05 alumina. The C-2000 samples were electrolytically etched in a solution of oxalic acid and HCl for 5-10 seconds. The B-3 samples were immersion etched in the same solution or in a solution of chrome-regia. The samples were examined under an inverted metallograph and digital camera at magnifications up to 500X.

## **Chapter 3 Results and Discussion**

### ***Weld Parameters***

#### **Root Pass**

Developing weld parameters for the root pass proved challenging and took the majority of the development time. This was due in part to the nature of an open root without any backing to support the molten weld puddle. Another challenge was the limited amount of material available for this research. These nickel alloys are expensive so the material supply for this research was limited. The number of virgin plates needed for the study was fixed, leaving only a small number of plates that could be used to develop weld parameters. When each of these test plates were used up, they would be cut apart, remachined, and welded again. This procedure was repeated until the best weld parameters were developed for each of the 3 nickel alloys. These nickel alloys are difficult to machine and this made the recycling process for the weldments very time consuming as well. The GMAW process using the Miller RMD<sup>®</sup> modified short circuit transfer mode was employed to determine if this alternative root weld process could provide the same quality and repeatability as the GTAW process. Two variables that seemed to have an important effect on the root pass quality were the root opening and root land. A smaller root land and a tapered root opening provided the best results. This

is thought to be due to less base material to melt initially as a balance must be struck with heat input into the weld. Too high of heat input would allow a melt through (blowout) and too little heat input would result in incomplete fusion on the root faces, Figure 15.

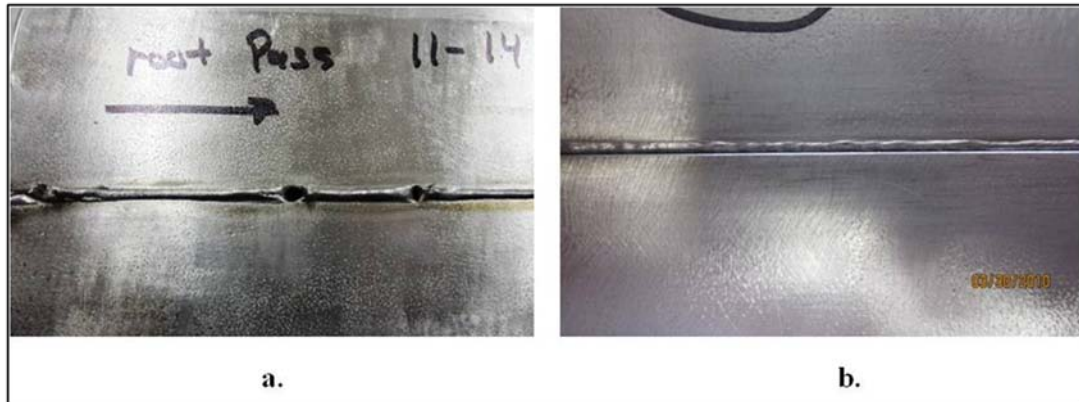


**Figure 15 Root Pass Defects; a. Melt-Through, b. Incomplete Fusion**

Initially tack welds were made at each end of the plates and the weld was started from one of the tack welds but blowout problems were a constant occurrence at the start of each root pass, generally within the first 1-2 inches. It is difficult for a puddle of molten metal to bridge the open air space of the root opening. The solution that proved successful was to eliminate the tack welds at each end and start the weld from one side of the bevel face and gradually travel down to the root land, bridge the opening and then continue down the center of the weld joint. This procedure provided the fewest melt-throughs and generally the best root fusion.

A faster travel speed, though counter intuitive, with approximately a 5° forward travel angle, also helped to give the best results. This was thought to be because it allowed more of the leading edge of the molten weld pool to fill and fuse with the root faces.

Three shielding gas mixtures were tried in the root pass development: 100% argon, 75% argon-25% helium, and 10% helium-0.4% CO<sub>2</sub>-balance argon. The same shielding gas

was used through the welding torch and also as a back purge on the root face. The 100% argon mixture gave a stable arc and good face cosmetics, (low oxidation), but did not give good root fusion. This was also true for the 75% argon-25% helium mixture as well. A stable arc and the best root fusion was provided by the 3 gas mixture, 10% helium-0.4% CO<sub>2</sub>-balance argon although the weld faces had more visible oxidation. The root passes for all 3 alloys were done at room temperature. All joint surfaces and an one inch wide strip on either side of the weld joint were cleaned with acetone before the start of each weld. The results of using the RMD<sup>®</sup> process were mixed. There were many successful root pass welds on all alloys and plate thicknesses, Figure 16.



*Figure 16 Complete Fusion Root Pass-view from back of the plate*

This is evidenced by the results of the mechanical tests and metallurgical examinations which appear in later sections of this chapter. That being said, there were a number of incomplete fusion root passes as well on both plate thicknesses and all alloys. This could

be explained by the RMD<sup>®</sup> waveform and parameters not being fully optimized. Also, currently this process seems to be too sensitive to small variations in parameters such as root opening and root land which make it not robust enough for the production environment at this time. The increased welding travel speed advantage and single weld process though may make pursuing further development of this process worthwhile. The final root pass weld process details and parameters for all 3 alloys are listed in Tables 4 & 5.

<b>Table 4 Root Pass General Welding Details- All Alloys</b>	
Robotic GMAW - RMD <sup>®</sup> Regulated Metal Deposition	
Power Supply - Miller Electric- Auto-Axcess 450	
0.045 inch Diameter Filler Wire - Specific to Each Alloy	
Wire Stick Out - 0.625 inch	
Shielding Gas - Torch and Back Purge - 10% Helium-0.4% CO2-Balance Argon	
All Root Passes - Room Temperature	
Position - Flat AWS 1G - 5° Travel Angle (Pull)	
Joint Geometry - Single V Groove, 70° Included Angle	
Root Land - All Alloys - 0.20 inch	
Root Opening (inches) - Taper in 10 inches- 0.25 Plate - 0.50 Plate	
	<b>C-2000:</b> .05-.06, .06-.07 inch
	<b>B-3:</b> .05-.06, .05-.08 inch
	<b>230:</b> .06-.07, .05-.06 inch

<b>Table 5 Root Pass Weld Parameters</b>							
<b>Alloy</b>	<b>Plate Thickness (inch)</b>	<b>Travel Speed (ipm)</b>	<b>Wire Feed Speed (ipm)</b>	<b>Avg Voltage</b>	<b>Avg Amperage</b>	<b>Arc Adjust (Trim)</b>	<b>Arc Control</b>
C-2000	0.25	20	225	15.4	135	54	26
	0.5	20	225	16.8	120	54	26
B-3	0.25	18	225	14	140	54	26
	0.5	18	225	15	128	54	26
230	0.25	18	225	16.5	128	54	26
	0.5	18	225	16.7	127	54	26

## **Fill Passes**

The development of weld parameters for the fill passes took less time than root pass development. This was due to the fact that the fill pass development did not have the challenge of an open root and since multiple weld passes were required to fill the groove, a greater number of welding variables could be tested before the test weldment had to be cut apart and remachined. The face of the root passed was lightly ground on all weldments before the first fill pass was made. A stainless steel wire brush was used to clean the welds and surrounding area from oxidation and any spatter between passes, no grinding was performed on the fill passes. The 0.25 inch thick plates required only 1 pass to fill the joint and the 0.50 inch thick plates required 5 fill passes. As a general statement, at the lower interpass temperatures of 100-300°F, the arc was more stable and the face of the weld had a smooth, even rippled texture. The higher interpass temperatures of 400 & 500°F seem to produce a more erratic arc, more spatter, and a weld face that was mottled in nature. Once acceptable weld parameters were obtained, they were maintained for consistency for all the fill passes on the thick plates. One interesting observation was that the first fill pass always had the highest amperage reading. This was favorable because it helped fuse the root pass. Fill pass 1 also had the smoothest weld face and a very stable arc, Figure 17.



*Figure 17 Typical Fill Pass 1*

Each succeeding pass had amperage levels going slightly lower with the same weld settings. The 3 shielding gas mixtures tested for the root pass were also tested on the fill passes. The shielding gas that produced the best arc characteristics and least oxidation was the 75% argon-25% helium mix for all 3 alloys. The welding wave form used in this study was developed for a 625 nickel alloy using a different shielding gas. Information from this study will be useful in developing a unique welding wave form for all of the study alloys which should improve welding performance. The fill pass weld parameters are listed below in Tables 6 & 7.

<b>Table 6 Fill Pass General Welding Details- All Alloys</b>
Robotic GMAW - Accu-Curve®
Power Supply - Miller Electric- Auto-Axcess 450
0.045 inch Diameter Filler Wire - Specific to Each Alloy
Wire Stick Out - 0.625 inch
Shielding Gas - 75% Argon-25% Helium
Position - Flat AWS 1G - Vertical Travel Angle
Joint Geometry - Single V Groove, 70° Included Angle

<b>Table 7 Fill Pass Weld Parameters</b>							
<b>Alloy</b>	<b>Plate Thickness (inch)</b>	<b>Travel Speed (ipm)</b>	<b>Wire Feed Speed (ipm)</b>	<b>Voltage Range</b>	<b>Amperage Range</b>	<b>Arc Adjust (Trim)</b>	<b>Arc Control</b>
C-2000	0.25	10	270	26-27	135-140	60	25
	0.5	12	270	26.5-28	140-160	60	28
B-3	0.25	10	250	24.5-25	125-135	54	25
	0.5	12	270	25-26	145-160	58	27
230	0.25	9	250	28-29	135-140	66	31
	0.5	9.5	250	27-28	120-140	64	30

## Mechanical Properties

### *Tensile Test*

Mechanical properties of the welds were evaluated using tensile tests performed on transverse weld specimens according to ANSI/AWS B4.0:2007 for the C-2000 and B-3 alloys. The results of these tests are listed in Tables 8 & 9.

<b>Table 8 Tensile Test C-2000</b>						
<b>0.25 inch Plate</b>						
<b>IT °F</b>	<b>Sample</b>	<b>Thickness</b>	<b>Width</b>	<b>Area in<sup>2</sup></b>	<b>UTS psi</b>	<b>Failure Location</b>
100	<b>1</b>	0.276	1.497	0.4132	103600	Center of Weld
	<b>2</b>	0.268	1.494	0.4004	110000	1 inch Below Weld
200	<b>3</b>	0.280	1.497	0.4192	110500	0.75 inch Below Weld
	<b>4</b>	0.277	1.497	0.4147	109700	Weld-Root Side
300	<b>5</b>	0.278	1.495	0.4156	109600	1 inch Above Weld
	<b>6</b>	0.258	1.505	0.3883	107000	Weld-Root Side
400	<b>7</b>	0.240	1.485	0.3564	109900	Weld-Root Side
	<b>8</b>	0.244	1.490	0.3636	107600	Weld-Root Side
500	<b>9</b>	0.283	1.507	0.4265	110100	Weld
	<b>10</b>	0.282	1.500	0.4230	107600	Weld-Root Side
<b>0.50 inch Plate</b>						
<b>IT °F</b>	<b>Sample</b>	<b>Thickness</b>	<b>Width</b>	<b>Area in<sup>2</sup></b>	<b>UTS psi</b>	<b>Failure Location</b>
100	<b>11</b>	0.498	0.904	0.4502	108900	1 inch Below Weld
	<b>12</b>	0.496	0.906	0.4494	107800	Weld-Root Side
200	<b>13</b>	0.496	0.907	0.4499	109200	Weld-Root Side
	<b>14</b>	0.500	0.905	0.4525	109600	Weld-Root Side
300	<b>15</b>	0.502	0.895	0.4493	107900	Weld-Root Side
	<b>16</b>	0.507	0.908	0.4604	108700	Weld
400	<b>17</b>	0.505	0.906	0.4575	108900	1.2 inches Above Weld
	<b>18</b>	0.502	0.905	0.4543	109900	1.3 inches Below Weld
500	<b>19</b>	0.500	0.905	0.4525	109300	1 inch Above Weld
	<b>20</b>	0.502	0.906	0.4548	109100	1.2 inches Above Weld

<b>Table 9 Tensile Test B-3</b>						
<b>0.25 inch Plate</b>						
<b>IT °F</b>	<b>Sample</b>	<b>Thickness</b>	<b>Width</b>	<b>Area in^2</b>	<b>UTS psi</b>	<b>Failure Location</b>
100	<b>21</b>	0.257	1.500	0.3855	131000	Weld
	<b>22</b>	0.256	1.502	0.3845	107200	Weld
200	<b>23</b>	0.257	1.500	0.3855	134900	Weld
	<b>24</b>	0.256	1.500	0.3840	134300	Weld
300	<b>25</b>	0.259	1.497	0.3877	120300	Weld-Root Side
	<b>26</b>	0.257	1.499	0.3852	131600	Weld
400	<b>27</b>	0.260	1.501	0.3903	119600	Weld-Root Side
	<b>28</b>	0.258	1.498	0.3865	123200	Weld
500	<b>29</b>	0.259	1.500	0.3885	101700	Weld-Root Repair
	<b>30</b>	0.256	1.500	0.3840	95000	Weld-Root Repair
<b>0.50 inch Plate</b>						
<b>IT °F</b>	<b>Sample</b>	<b>Thickness</b>	<b>Width</b>	<b>Area in^2</b>	<b>UTS psi</b>	<b>Failure Location</b>
100	<b>31</b>	0.506	0.907	0.4589	125000*	*did not break - jaw failure
	<b>32</b>	0.506	0.670	0.3390	129200	Weld
200	<b>33</b>	0.508	0.704	0.3576	128100	Weld
	<b>34</b>	0.507	0.675	0.3422	128100	Weld
300	<b>35</b>	0.507	0.710	0.3600	128600	Weld
	<b>36</b>	0.509	0.714	0.3634	128200	Weld
400	<b>37</b>	0.507	0.715	0.3625	127600	Weld
	<b>38</b>	0.508	0.706	0.3586	127700	Weld
500	<b>39</b>	0.507	0.708	0.3590	127400	Weld
	<b>40</b>	0.508	0.709	0.3602	118100	Weld-Root Side

All tensile failures were ductile for both alloys and plate thicknesses, Figure 18. All Ultimate Tensile Strengths (UTS) for the C-2000 alloy showed no significant drop due to interpass temperature and all were above the ASME Boiler and Pressure Vessel Code Section IX minimum 100,000 psi for UTS [45].

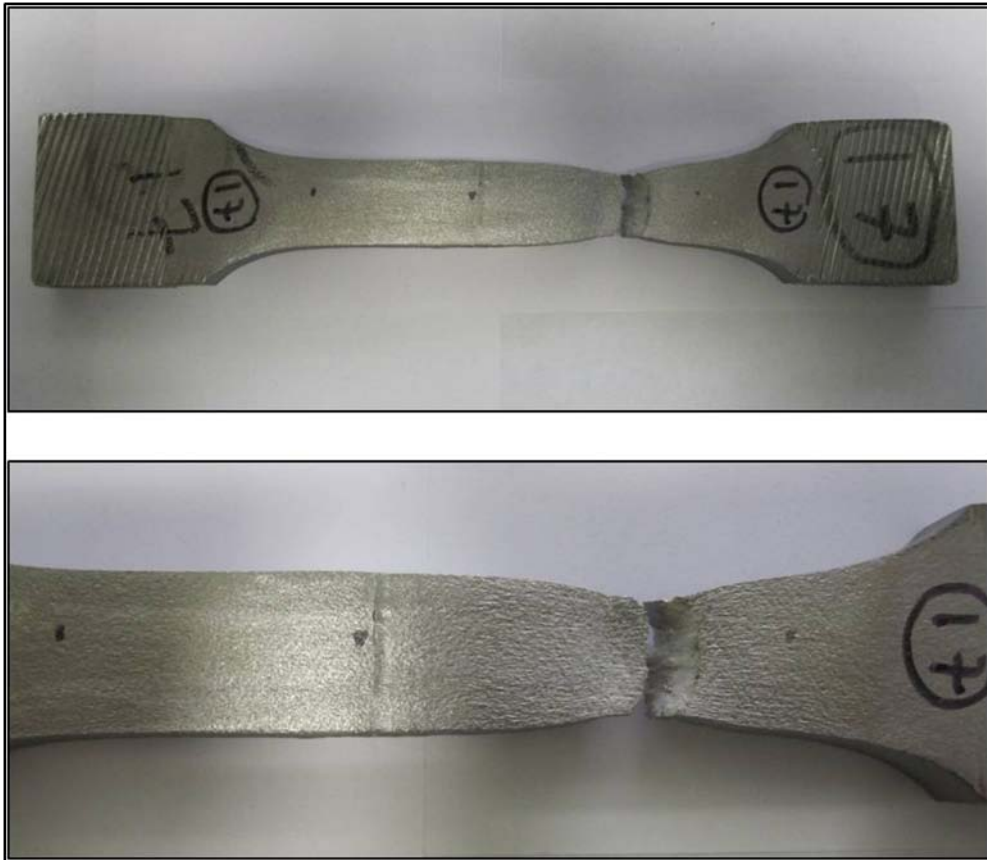


*Figure 18 Top-Typical Tensile Break C-2000, Bottom- Close Up of Tensile Break*

Most samples broke in the weld and many of the tensile failures originated on the root side. This was a common occurrence for both alloys and could be attributed to lack of fusion on the root faces from the original root pass weld. The B-3 showed similar results but the lack of fusion in the root was more pronounced in these specimens. Upon reviewing the weld processing notes, many of the root passes were plagued with a root pass that started with good fusion and finished with severe lack of root penetration and fusion. This could be attributed to weld parameters that were not optimized since these tensile failures occurred on the root side. Figure 19 shows the typical lack of fusion defect starting on the root side of the weld during the tensile tests.

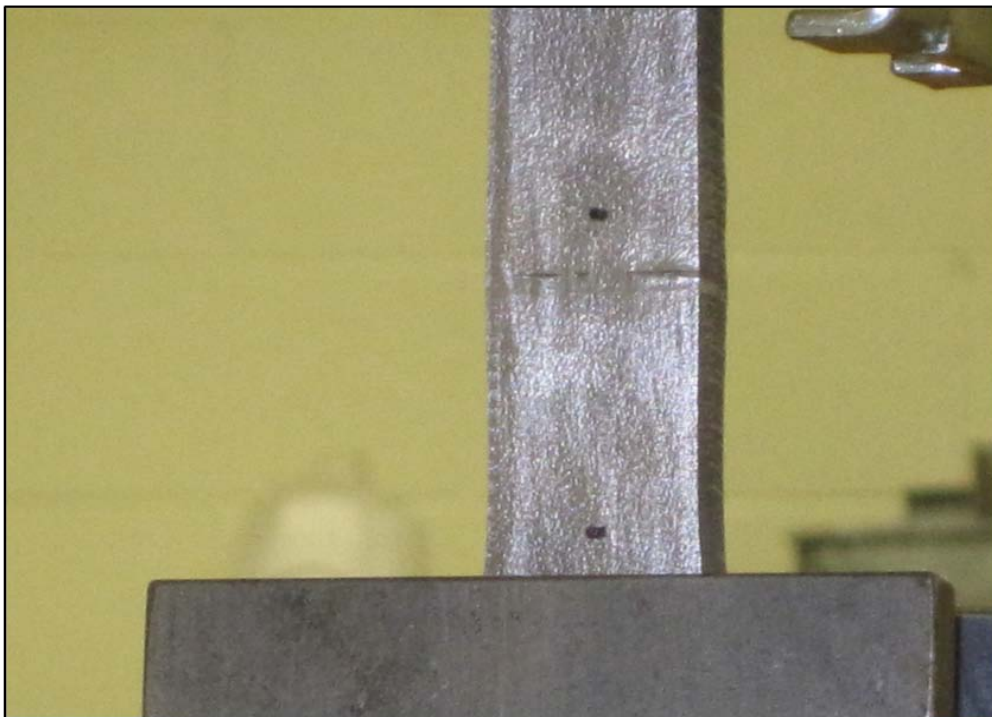


*Figure 19 Start of Tensile Failure -Lack of Root Fusion*

If the lack of root fusion is discounted for the B-3 alloys as well, the UTS's were above the 110,000 psi ASME Boiler and Pressure Vessel Code Section IX minimum for all interpass temperatures. The B-3 alloys were the strongest in terms of tensile strengths as evidenced by sample 31 which did not break and instead broke a gripping jaw of the tensile tester. The cross sectional area was reduced for the remaining tensile samples because of this. Samples 29 and 30 had severe lack of root penetration and fusion, Figure 20, and were repaired with GTAW. The increased heat input and weld cycles could have decreased ductility and be the reason for the significantly lower UTS values.



*Figure 20 B-3 Sample 30 - Root Pass -Lack of Penetration*

The tensile test results are summarized in the graphs below, Figures 21 & 22.

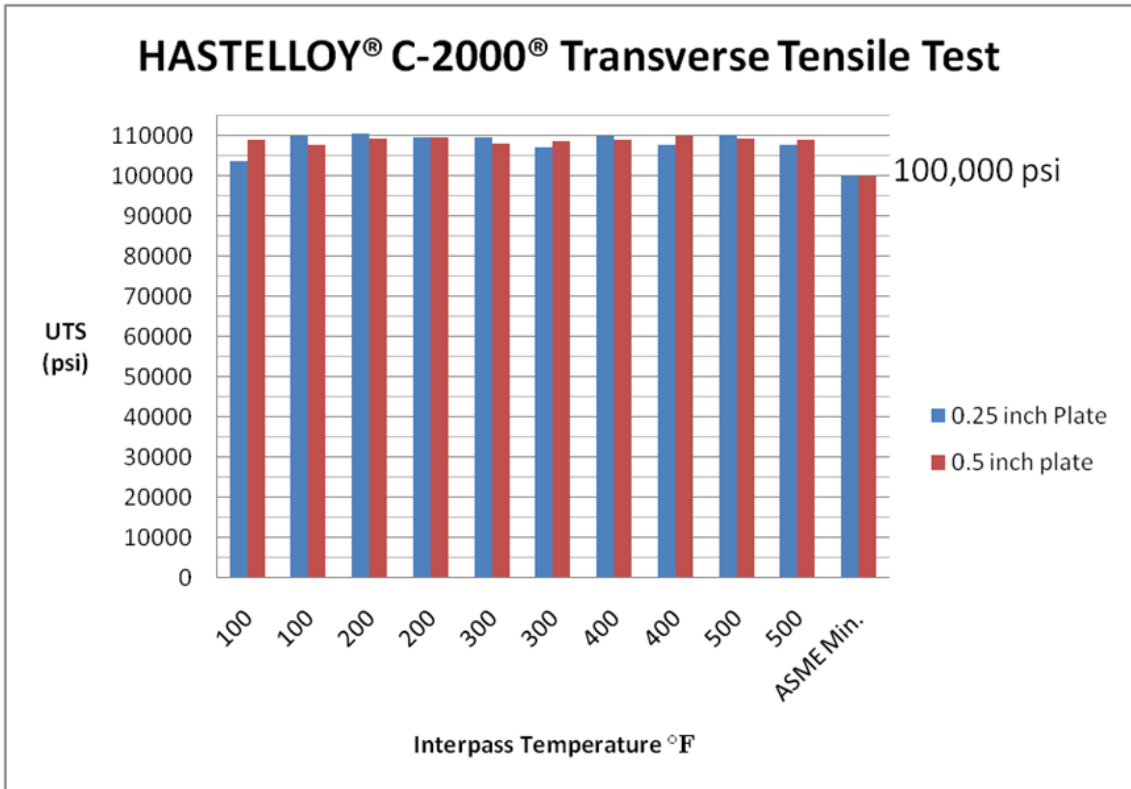


*Figure 21 C-2000 Tensile Test Summary*

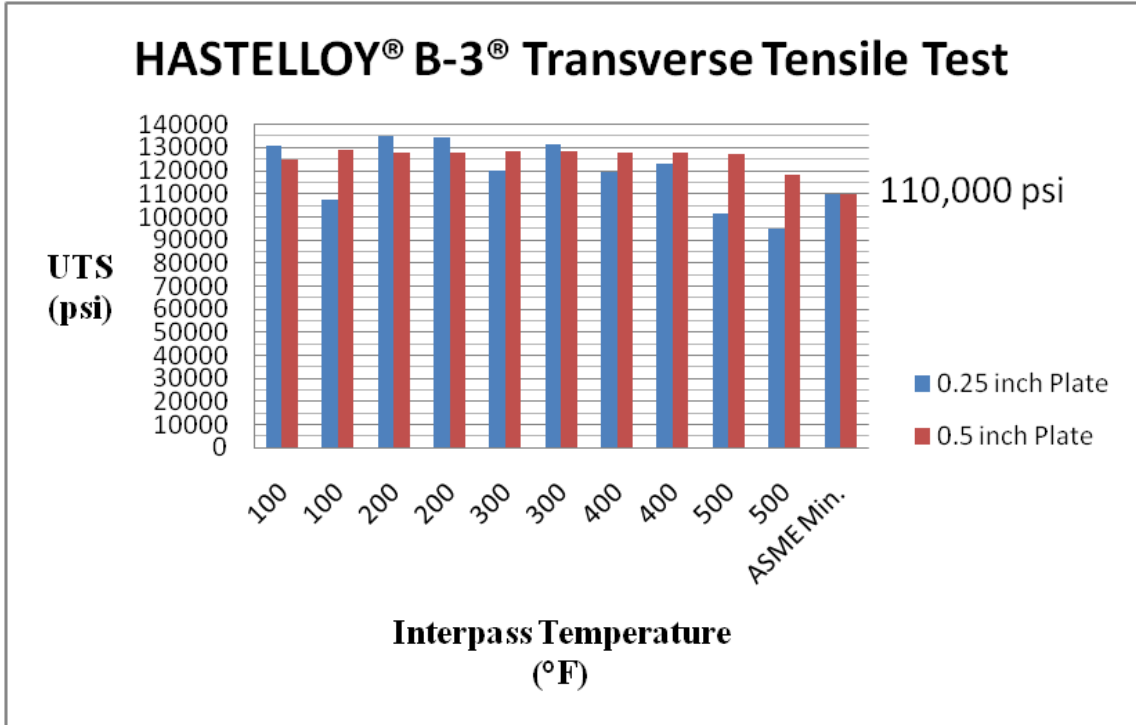


*Figure 22 B-3 Tensile Test Summary*

The C-2000 transverse tensile tests all exceeded the 100 ksi minimum UTS for plate as required by Section IX of the 2007 ASME Boiler and Pressure Vessel Code [45]. This was true even for the weldments with root penetration defects. The C-2000 alloys were also the easiest to weld. The transverse tensile test results for the B-3 alloy exceeded the 110 ksi ASME minimum UTS for plate when the three specimens with incomplete root fusion are discounted.

**Guided Bend Tests**

Transverse weld guided bend test were performed in accordance with ANSI/AWS

B4.0:2007 on the C-2000 and B-3 alloys. The results are shown in Tables 10 & 11.

<b>Table 10 2T Transverse Guided Bend Tests C-2000 Alloy</b>							
<b>0.25 inch Thick Plates</b>				<b>0.5 inch Thick Plate</b>			
<b>IT °F</b>	<b>Sample</b>	<b>Face</b>	<b>Root</b>	<b>Sample</b>	<b>Face</b>	<b>Root</b>	<b>Side</b>
100	<b>1</b>	Pass	Fail	<b>11</b>	Pass	Fail	Pass
	<b>2</b>	Pass	*	<b>12</b>	Pass	Fail	Fail
200	<b>3</b>	Pass	Pass	<b>13</b>	Pass	Fail	Fail
	<b>4</b>	Pass	Fail	<b>14</b>	Pass	Pass	Fail
300	<b>5</b>	Pass	Fail	<b>15</b>	Pass	Fail	Fail
	<b>6</b>	Pass	Pass	<b>16</b>	Pass	Fail	Fail
400	<b>7</b>	Pass	Fail	<b>17</b>	Pass	Pass	Pass
	<b>8</b>	Pass	Fail	<b>18</b>	Pass	Pass	Pass
500	<b>9</b>	Pass	Fail	<b>19</b>	Pass	Pass	Pass
	<b>10</b>	Pass	Pass	<b>20</b>	Pass	Pass	Pass

\*Short Material on Weldment

<b>Table 11 2T Transverse Guided Bend Tests B-3 Alloy</b>							
<b>0.25 inch Thick Plates</b>				<b>0.5 inch Thick Plate</b>			
<b>IT °F</b>	<b>Sample</b>	<b>Face</b>	<b>Root</b>	<b>Sample</b>	<b>Face</b>	<b>Root</b>	<b>Side</b>
100	<b>21</b>	Pass	Pass	<b>31</b>	Pass	Pass	Pass
	<b>22</b>	Pass	Fail	<b>32</b>	Pass	Fail	Pass
200	<b>23</b>	Pass	Pass	<b>33</b>	Pass	Pass	Pass
	<b>24</b>	Pass	Pass	<b>34</b>	Pass	Pass	Pass
300	<b>25</b>	Pass	Fail	<b>35</b>	Pass	Pass	Pass
	<b>26</b>	Pass	Pass	<b>36</b>	Pass	Fail	Pass
400	<b>27</b>	Pass	Pass	<b>37</b>	Pass	Pass	Pass
	<b>28</b>	Pass	Pass	<b>38</b>	Pass	Pass	Fail
500	<b>29</b>	Pass	Fail	<b>39</b>	Pass	Fail	Pass
	<b>30</b>	Pass	Fail	<b>40</b>	Pass	Fail	Pass

The bend tests seem to reinforce the tensile test results. All the transverse *face* bend tests were passed by *both* alloy groups and *both* plate thicknesses at *all* interpass temperatures. This would seem to indicate good weld fusion, soundness, and ductility from the all the fill pass welds. Figure 23 shows typical specimens that passed the requirements of the AWS guided bend test.



*Figure 23 Bend Test Specimens that Passed the AWS Bend Test,-Face, Root, & Side*

The transverse root and side bend tests were a mix of pass and fails throughout the interpass temperature range for both alloys. This would also seem to point to lack of penetration and fusion from a non-optimized root weld pass as the previous tensile tests have supported. Most failures had small cracks on or near the root face. Samples 29 & 30, B-3, 0.25 inch thick specimens, had gross failures as shown in Figure 24. As reported earlier, this may have been due to repairs to the root pass which may have precipitated undesirable carbide formation in the HAZ. This would seem to indicate that the root and side bend test specimen failures can be attributed to process optimization problems and not because of the higher inter pass temperatures.

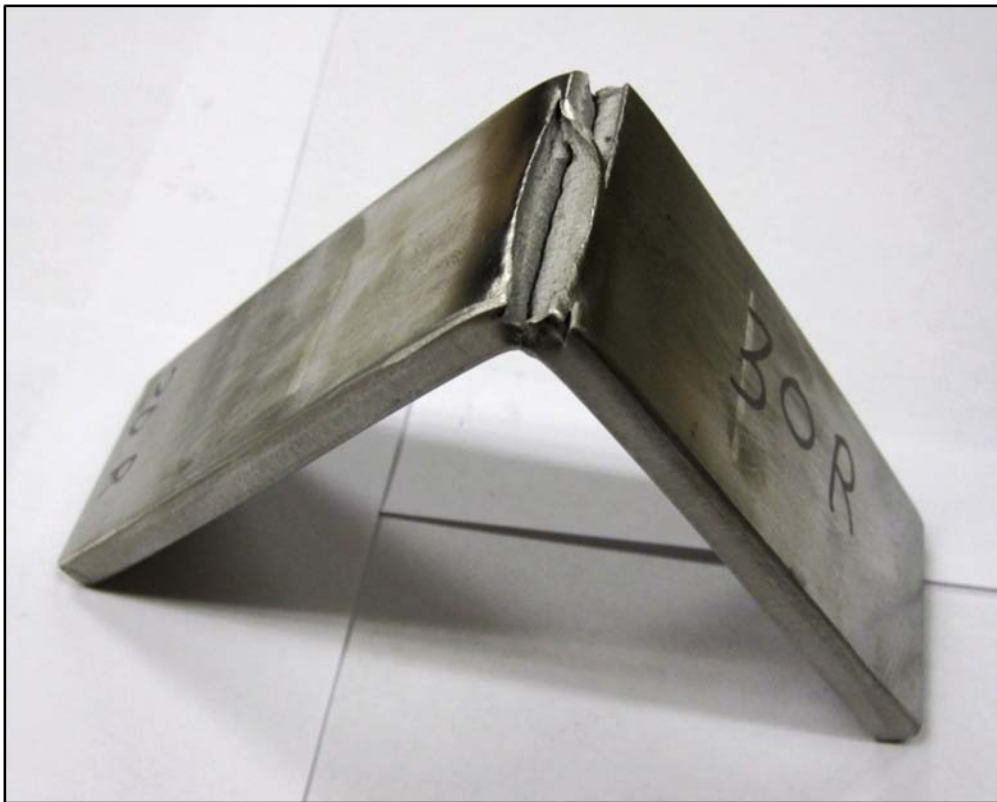


*Figure 24 Alloy B-3 Sample 30 Root Bend Failure*

### ***Hardness Testing***

Rockwell hardness tests, B scale (RHB) were performed on samples cut transversely across the weld in the base metal and weld areas as shown in Figure 25. The average of three readings for both alloys is reported in Tables 12 and 13.

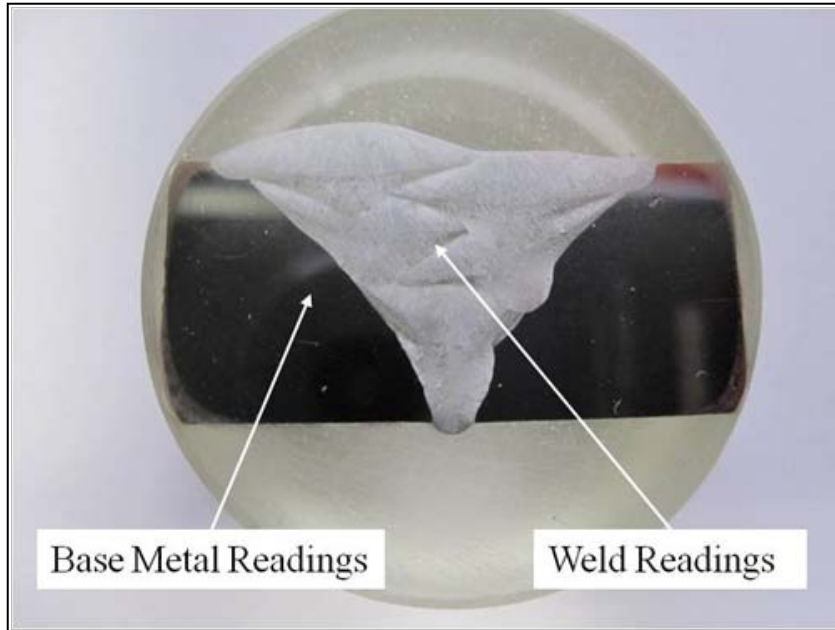


***Figure 25 Rockwell Hardness Reading Areas***

<b>Table 12 Alloy C-2000 Hardness</b>			
<b>0.25 inch Plate</b>		<b>RHB</b>	
<b>IT °F</b>	<b>Sample</b>	<b>Base Metal</b>	<b>Weld</b>
100	2	89.6	91.7
200	3	90.1	91.2
300	5	89.2	91.7
400	7	89.6	92.0
500	10	88.5	91.4
<b>0.50 inch Plate</b>		<b>RHB</b>	
<b>IT °F</b>	<b>Sample</b>	<b>Base Metal</b>	<b>Weld</b>
100	11	87.2	95.1
200	14	87.3	94.1
300	15	84.9	93.1
400	18	86.1	93.7
500	19	86.3	92.9

<b>Table 13 Alloy B-3 Hardness</b>			
<b>0.25 inch Plate</b>		<b>RHB</b>	
<b>IT °F</b>	<b>Sample</b>	<b>Base Metal</b>	<b>Weld</b>
100	22	97.1	94.5
200	23	97.5	94.5
300	25	97.3	93.6
400	28	96.7	92.8
500	29	97.6	95.4
<b>0.50 inch Plate</b>		<b>RHB</b>	
<b>IT °F</b>	<b>Sample</b>	<b>Base Metal</b>	<b>Weld</b>
100	31	93.2	97.0
200	34	93.2	96.6
300	36	93.7	96.0
400	38	92.0	95.3
500	40	92.7	95.9

The Rockwell hardness tests do not show any significant change through the range of interpass temperatures for both alloys. Readings for both alloys ranged from the mid 80's to the mid 90's on the B scale. The C-2000 alloy shows a slightly higher hardness reading in the weld as compared to the base metal region but this is to be expected since the weld region has melted and re-solidified. These differences range from 2-7 points and can be considered small. The same result was found for the 0.5 inch thick plates of alloy B-3. The 0.25 inch thick plates of B-3 had a slightly higher hardness in the base metal as compared to the weld but this may be explained by compositional differences, fewer weld passes, (less heat input), and the plate processing since it is thinner and the cold work effect from rolling may be more pronounced through the thinner cross section.

### ***Weldment Corrosion Testing***

The results of the corrosion tests are summarized in Figures 26 and 27. The corrosion rate in mils per year, mpy, does not have much significance for welded material but the tests do provide a severe corrosion environment to check for Intergranular Attack, IGA. Generally the weld metal is more susceptible to IGA than the wrought material because of a tendency for the alloying elements to segregate and solidify along the grain boundaries during welding. The corrosion rate raw data for both alloys is shown below for informational purposes only.

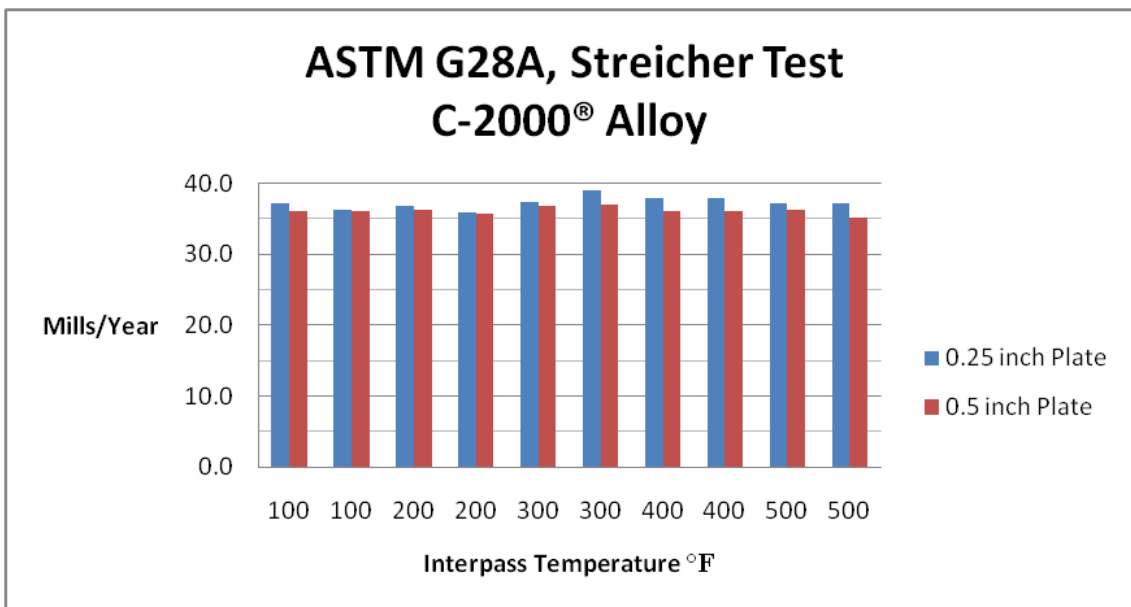


***Figure 26 ASTM G28A Corrosion Test Results***

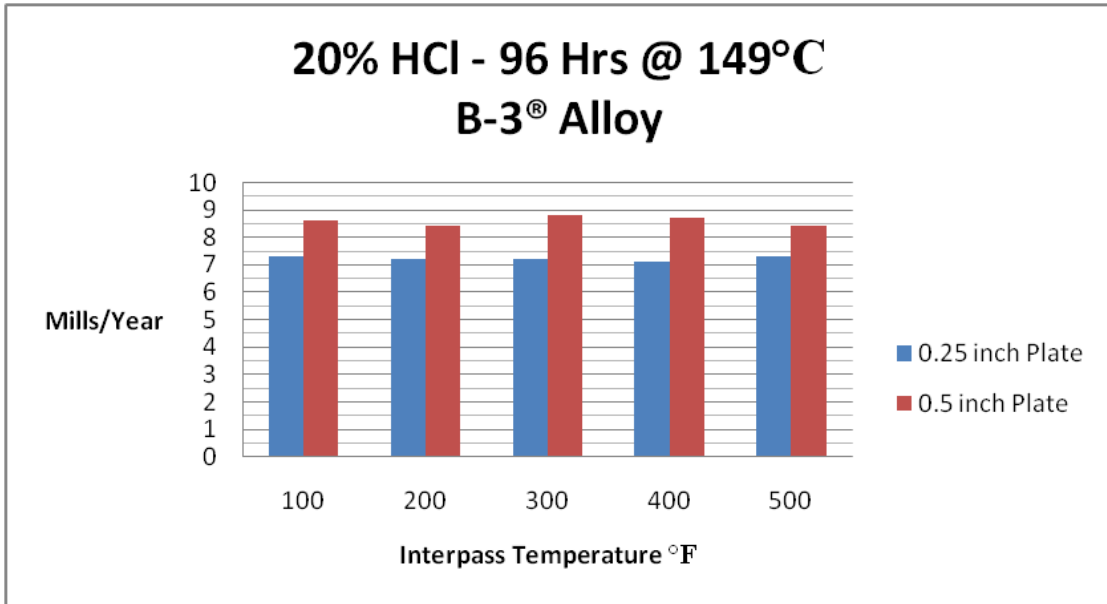


*Figure 27 20% HCl Corrosion Test Results*

Figure 28 shows two transverse weld specimens after the immersion corrosion tests.



*Figure 28 Corrosion Test Specimens, a. 0.5 inch C-2000 , b. 0.5 inch B-3*

When the corrosion testing was finished, transverse weld specimens at 200 & 500°F interpass temperatures for both alloys were metallurgically examined for corrosion attack along the weld zone on the face and root. The results are reported in Tables 14 and 15.

<b>Table 14</b>			
<b>C-2000 Weldment Corrosion</b>			
<b>ASTM G28A/A262B</b>			
<b>IT °F</b>	<b>Sample</b>	<b>Maximum Corrosion Depth in mils</b>	<b>Location</b>
200	14	1.3	Root
500	10	1	Root
500	20	0.4	Root

<b>Table 15</b>			
<b>B-3 Weldment Corrosion</b>			
<b>20% HCl @ 149°C for 96 Hrs.</b>			
<b>IT °F</b>	<b>Sample</b>	<b>Maximum Corrosion Depth in mils</b>	<b>Location</b>
200	23	1.4	Root
500	39	0.7	Root

Depth of corrosion attack that is less than 7 mils (0.18mm) is generally considered acceptable [47]. The maximum depth of corrosion attack for the 500°F samples for both alloys is less than 2 mils (0.05mm). This would seem to indicate that the higher interpass temperature does not adversely affect the alloys resistance to corrosion along the weld zone.

Representative micrographs from the transverse sectioned weldments are shown below.

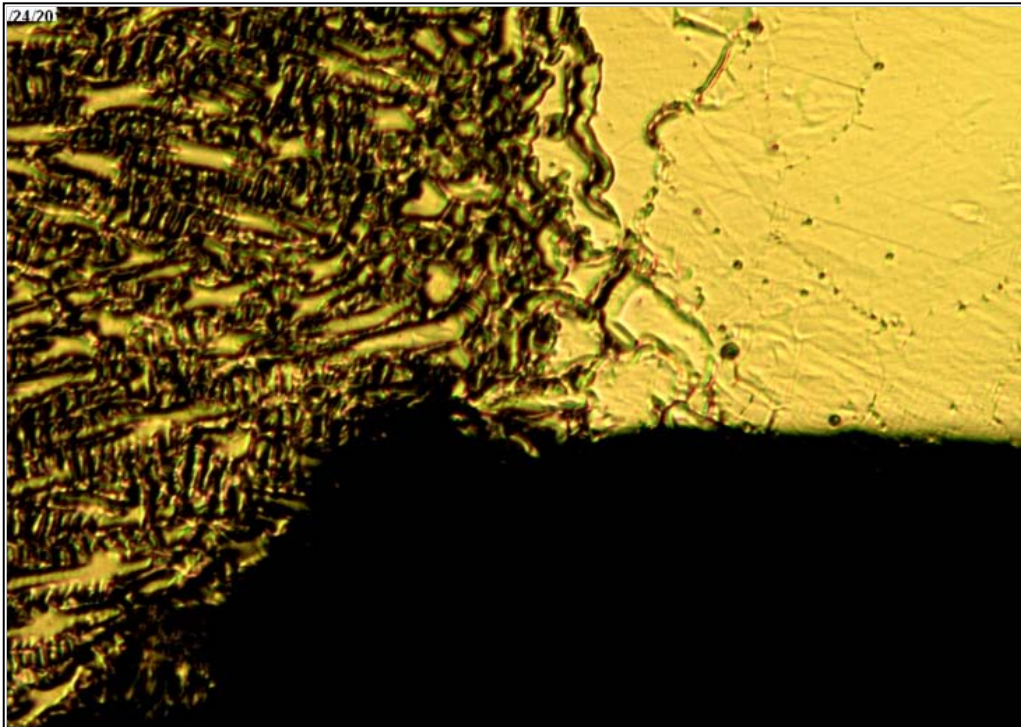


*Figure 29 C-2000 500°F IT Root Corrosion Attack 200X*

Figure 29 shows the maximum corrosion attack in the weld region of the root pass (0.4 mils) for alloy C-2000 at interpass temperature of 500°F. The B-3 weldment at 500°F interpass temperature shows no attack on the weld face, Figure 30, and minimal attack in the HAZ of the root, Figure 31. Corrosion attack in the HAZ of the root at 200°F interpass temperature, B-3 alloy is shown for comparison purposes in Figure 32. Figure 33 shows the corrosion attack for incomplete root fusion along the weld and base metal boundary. This was a common result for both alloys and would be expected for incomplete root fusion, a crevice defect. Also of note, is the minimal attack in the HAZ region of the root.

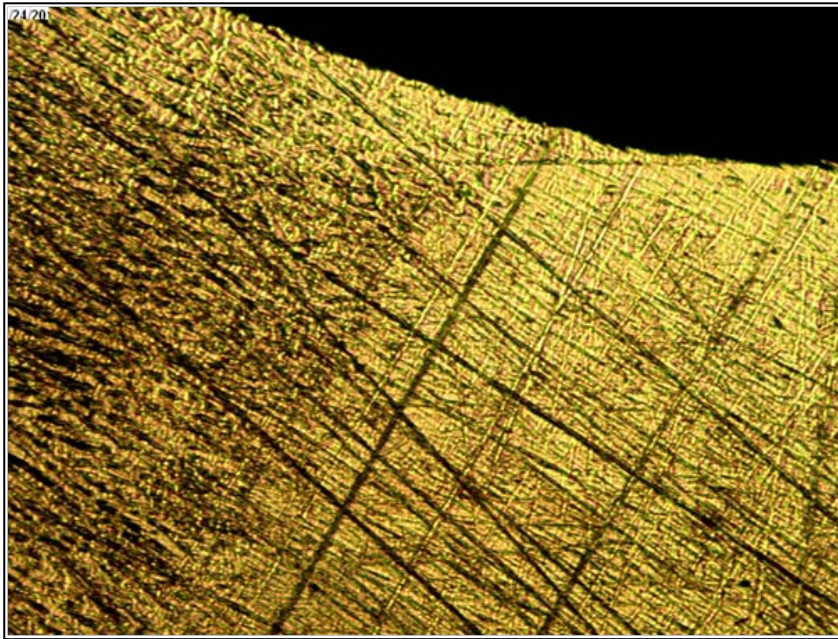


*Figure 30 B-3 500°F IT Weld Face – No Measurable Corrosion Attack*

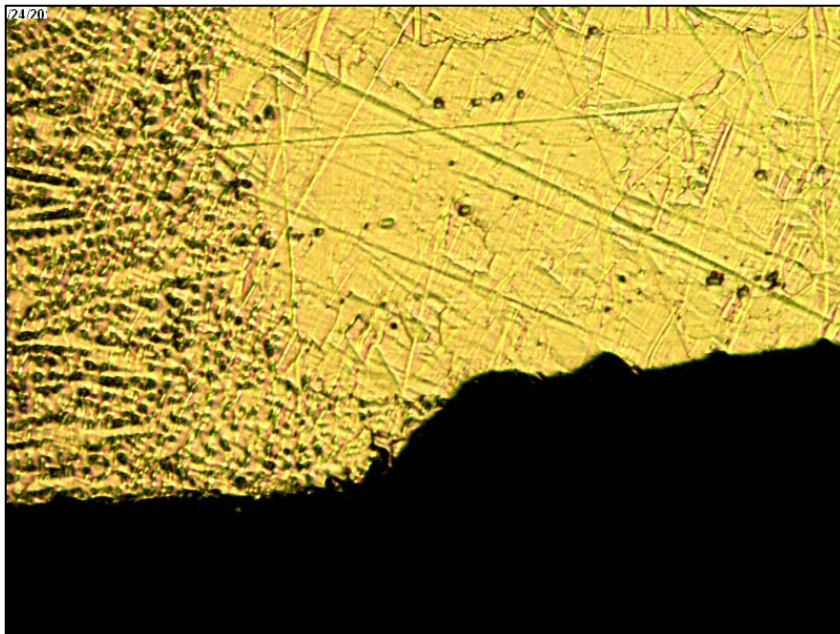


*Figure 31 B-3 500°F IT HAZ Root Corrosion 100X*

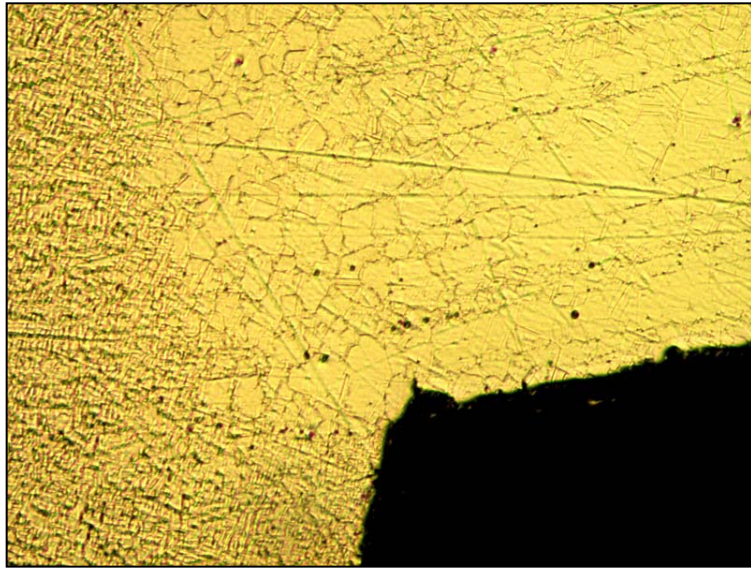


*Figure 32 B-3 200°F IT HAZ Corrosion at Root 100X*

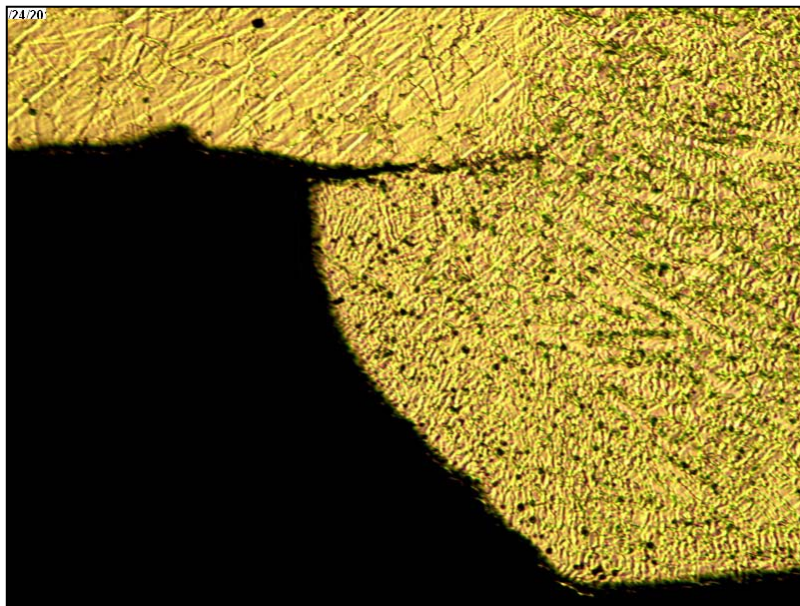


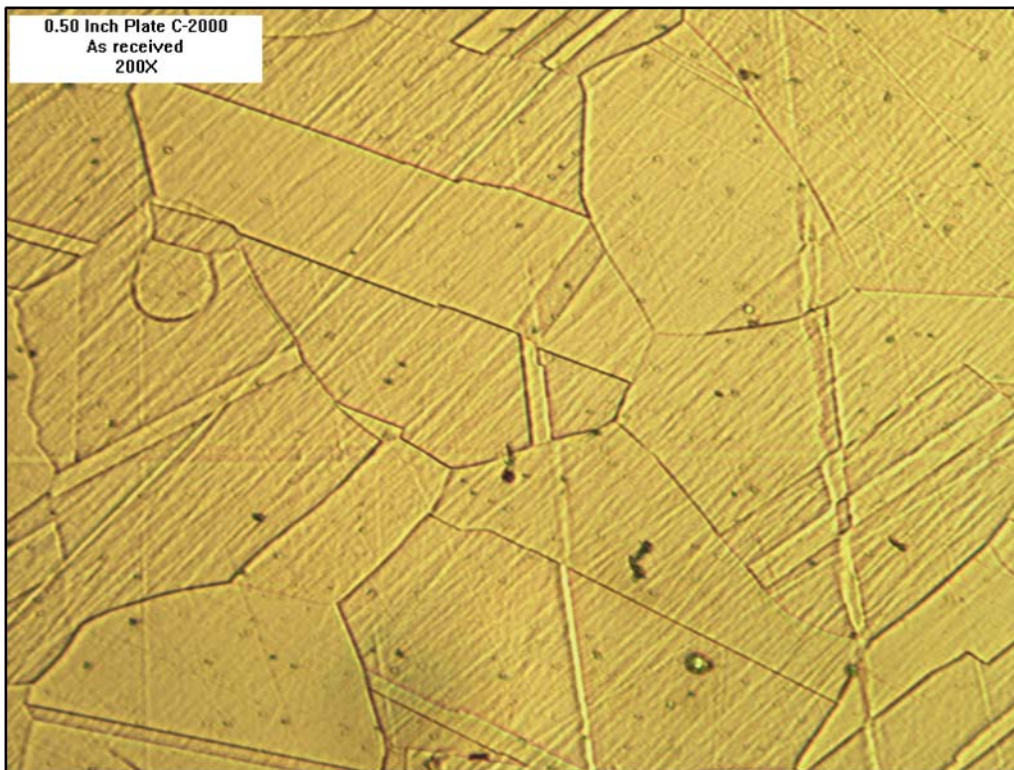
*Figure 33 B-3 200°F IT -Incomplete Root Fusion  
-Corrosion Attack 100X*

The maximum depth of attack along the weld, face and root, for either alloy, both plate thickness was less than 2 mils (0.05mm). These results would seem to indicate that the higher interpass temperature of 500°F did not increase the depth of corrosion attack along the weld for either the C-2000 or B-3 alloys.

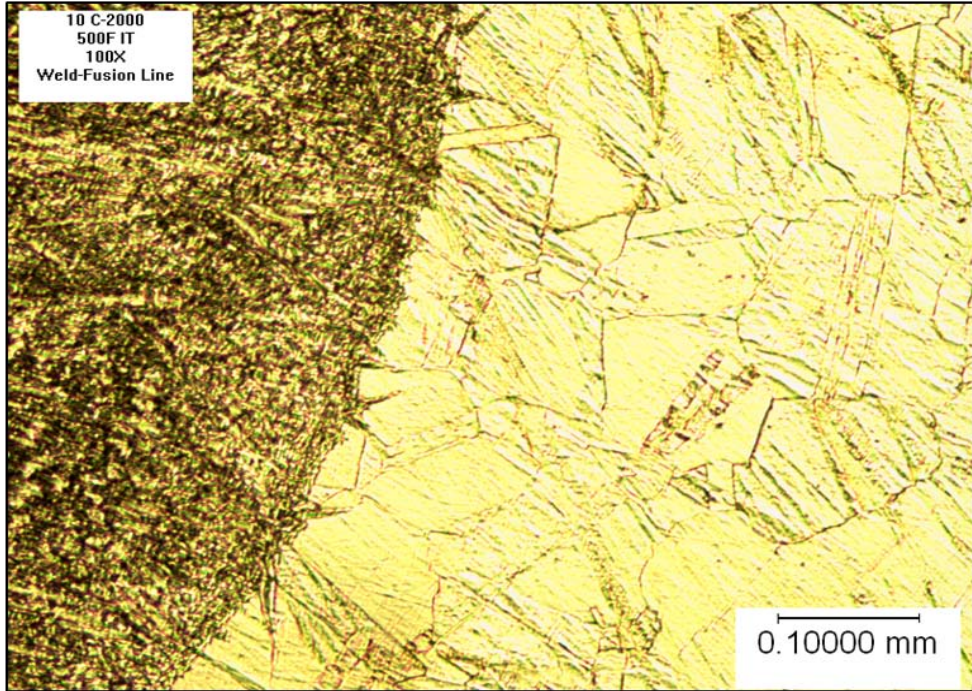
### ***Weld Microstructure and Metallography***

Transverse weld specimens were examined under a light microscope for weld defects such as lack of fusion and cracking. The microstructure was also examined for any change in grain structure or undesirable carbide formation by comparing it to the as received material and base material of the weldment. Representative alloy micrographs are shown below.

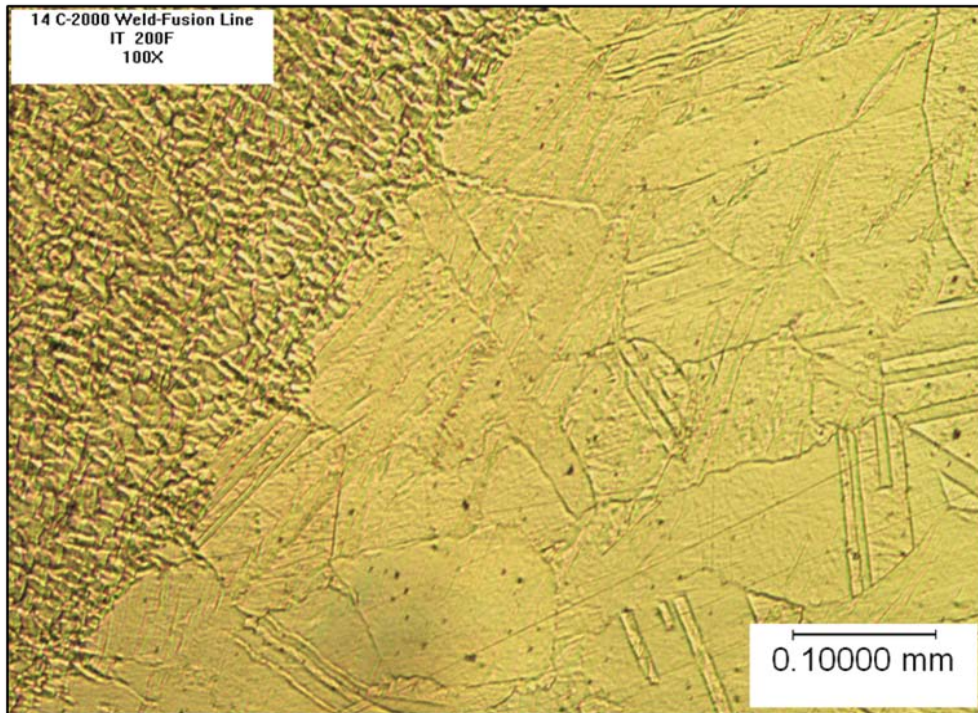
### **C-2000 Alloy**



*Figure 34 C-2000 0.50 inch Plate - As Received*



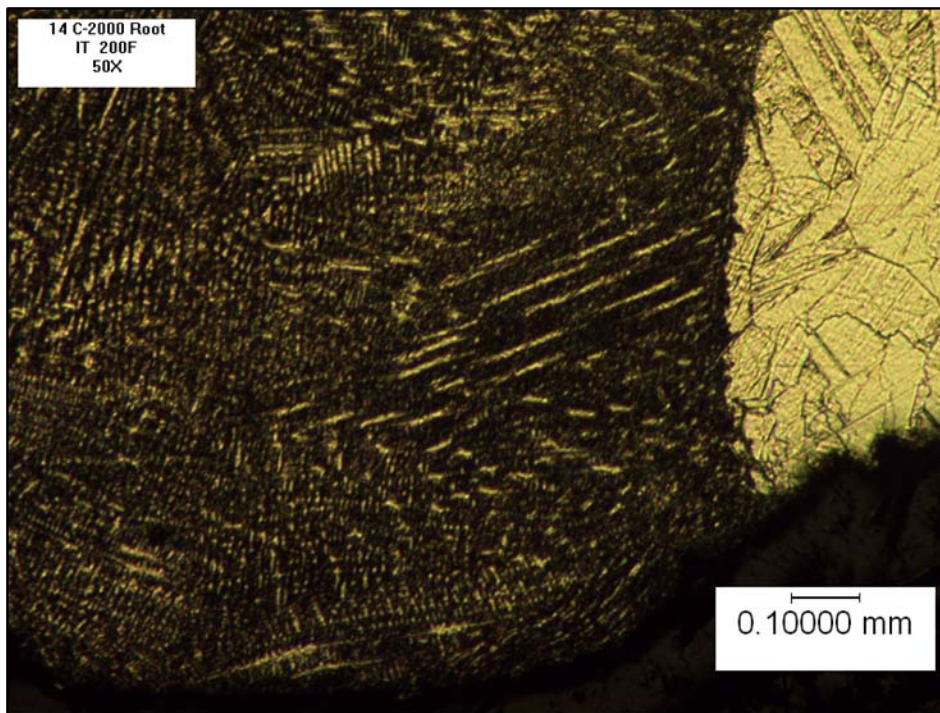
*Figure 35 C-2000 0.25 inch plate 500°F Interpass Temperature Weld-Fusion Boundary*



*Figure 36 C-2000 0.50 inch plate 200°F Interpass Temperature Weld-Fusion Boundary*

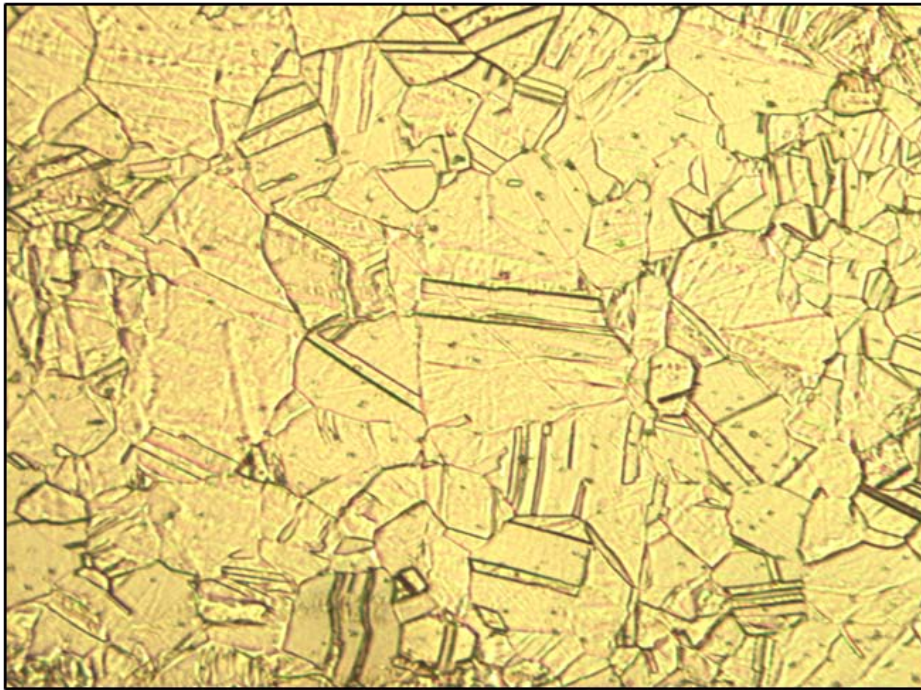
The micrographs above show a good weld fusion boundary and penetration and no undesirable carbide formations at interpass temperatures of 500°F, Figure 35. The microstructure at 500°F is similar to that at 200°F interpass temperature, Figure 36, and to the as received microstructure, Figure 34 as well. This reinforces the results of the tensile and bend tests that the higher interpass temperature did not have an effect on the mechanical properties of the weldment and no undesirable phases were precipitated in the HAZ.

Figure 37 shows a good root fusion boundary.



*Figure 37 C-2000 0.50 inch plate 200°F Interpass Temperature Root Fusion*

**B-3 Alloy**



*Figure 38 B-3 Representative Microstructure 100X*

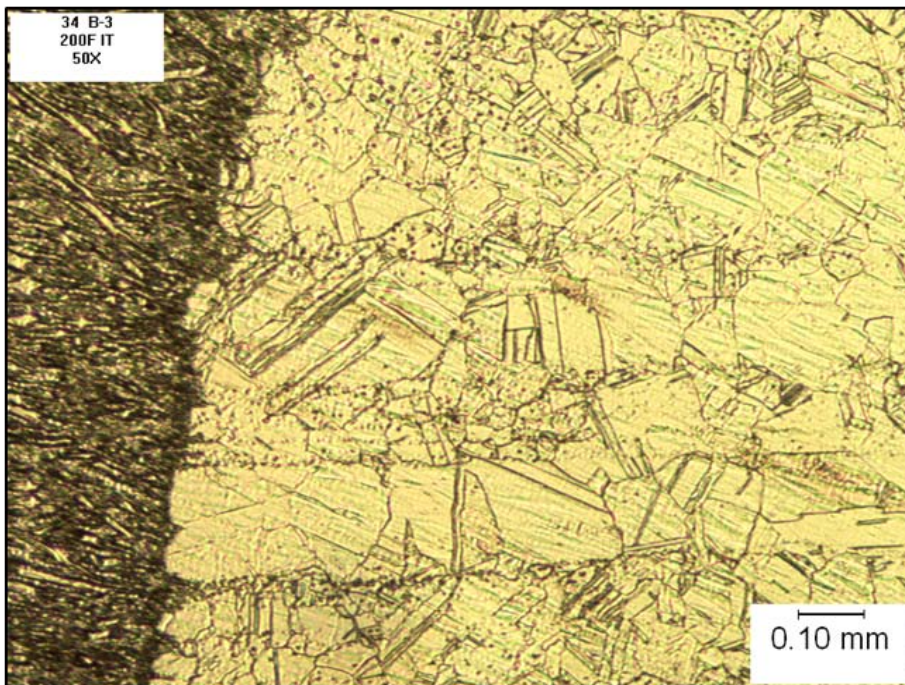


*Figure 39 B-3 0.5 inch Plate 200°F Interpass Temperature Weld-Fusion Boundary*

Figure 40 shows a defect that was common to both alloys and plate thicknesses over the entire range of interpass temperatures, lack of root fusion.

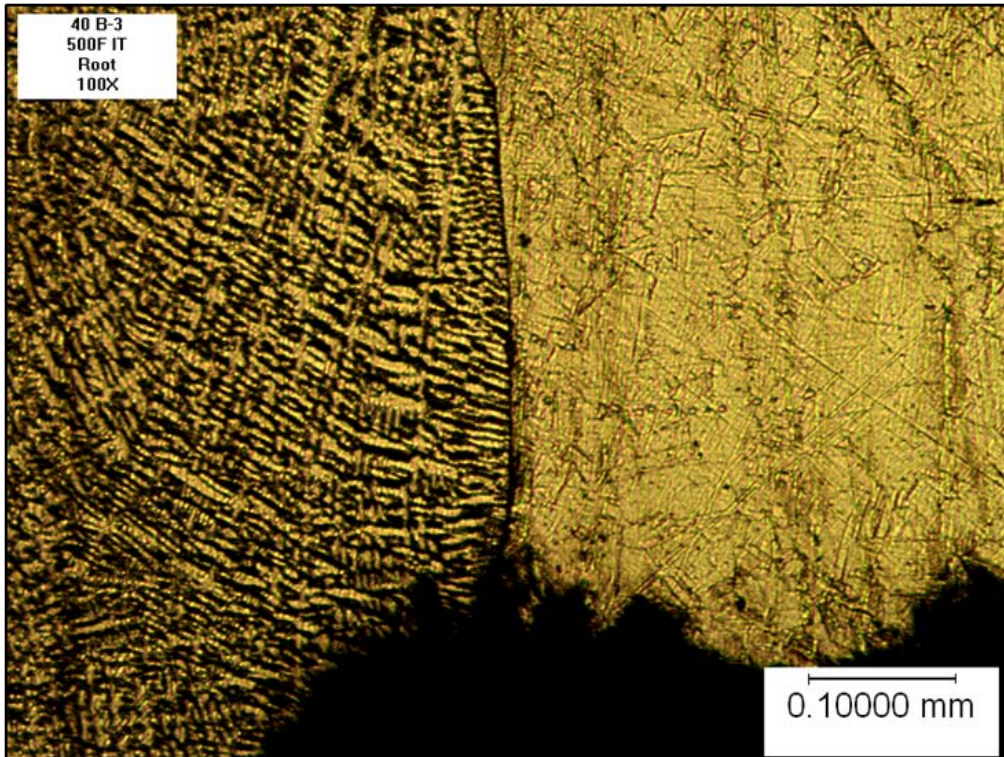


*Figure 40 B-3 0.5 inch Plate 500°F Interpass Temperature Lack of Root Fusion*

This is thought to come from the non-optimized weld parameters during the root pass.

Also a lack of fusion defect was found on sample 40, a B-3 alloy, 0.5 inch plate, 500°F interpass temperature, at weld fill pass 1. The defect occurred along the fusion boundary and was approximately 0.035 inch (0.9mm) long, Figure 41.

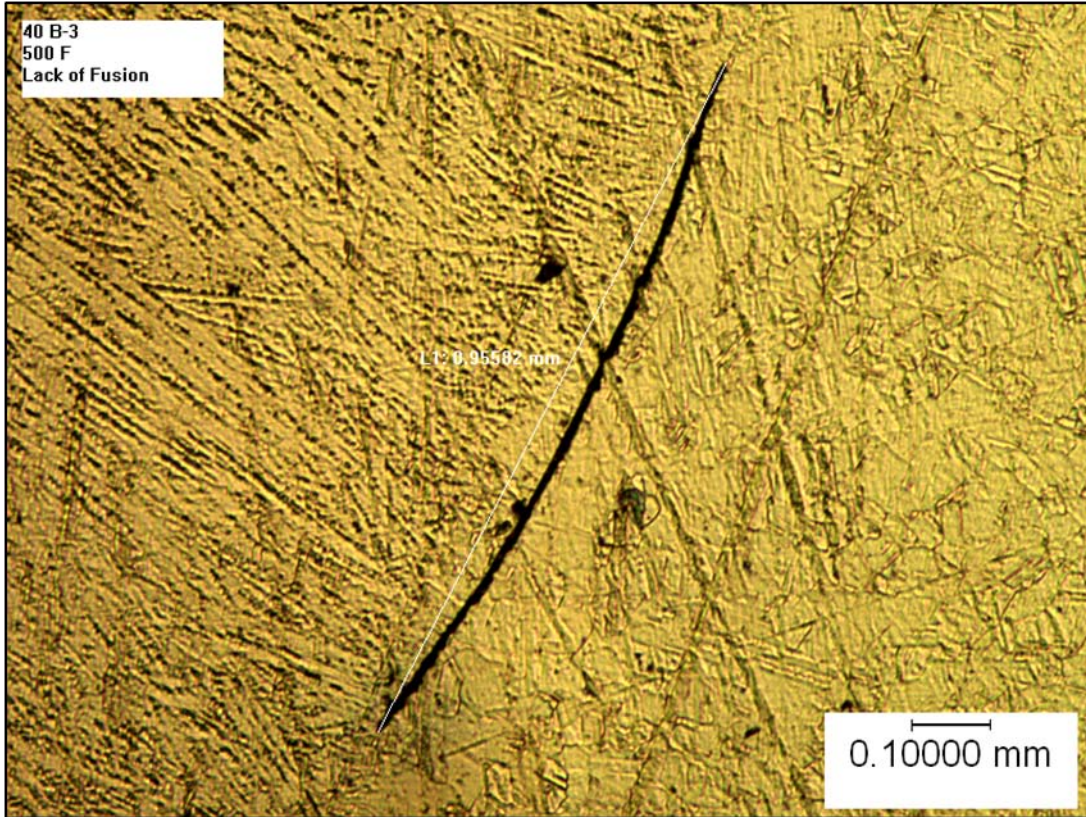


*Figure 41 B-3 0.5 inch Plate 500°F Interpass Temperature Lack of Fusion*

This small lack of fusion defect was not seen in any other weld cross section and could be from a welding process issue. A characteristic of the molten nickel weld puddle is low fluidity and low penetration. Under certain weld joint geometries such as steep toe angle with the wall, the weld puddle may require some additional weld torch manipulation. A stringer weld bead, no side-to-side manipulation, was used to keep heat input low, this may have caused the lack of fusion defect seen in sample 40.

The micrographs of both alloys do not show a change of microstructure at the higher interpass temperatures. All the test samples passed the tensile and bend tests indicating that the interpass temperature can vary from 100-500°F without harming the ability of the weldment to perform at the level of the parent alloy with respect to UTS, weld ductility and weld soundness. The examination under the light microscope at magnifications to 500X did not reveal any undesirable phases in the HAZ or weld cracking.

## **Chapter 4 Conclusions**

This dissertation presented research on the effect of interpass temperature on two nickel alloys; HASTELLOY C-2000 and HASTELLOY B-3. Welding parameters were also developed for these alloys and also for HAYNES 230 alloy using the Gas Metal Arc Welding, GMAW, as a single process for both the root and fill weld passes. A variety of tests were performed to evaluate the mechanical performance and corrosion characteristics of these alloys. Based on these tests the following was concluded:

1. Interpass temperatures of 100 through 500°F had no significant effect on the transverse tensile strength of the HASTELLOY C-2000 and HASTELLOY B-3 Alloys. All ultimate tensile strengths for both alloys were above the ASME Boiler and Pressure Vessel Code Section IX minimum.
2. No significant corrosion attack was found along the weld, face or root sides, for both alloys at the higher interpass temperature of 500°F.
3. No weld cracking or deleterious effect on the microstructure was found at the higher interpass temperatures.

4. Using the GMAW process as a sole process in the multipass welding of these alloys including HAYNES 230 alloy is possible and shows promise. Although it should be noted that the root pass was sensitive to process variables and lack of root fusion was a common defect over all temperatures, plate thicknesses, and alloys.
5. Robotic weld parameters using a digital power supply were developed and gave sound welds for these alloys.

These results are important because they represent the first systematic study of the interpass temperature variable for HASTELLOY C-2000 and HASTELLOY B-3 alloys and this research has shown that interpass temperatures up to 500°F are possible in the welded fabrication of these alloys. These original findings should benefit fabricators of these nickel alloys as well as the welding community in general.

## **Chapter 5 Study Limitations**

The results of the research done here were not intended to define a complete welding procedure specification (WPS) as defined by the welding codes such as the ASME Boiler and Pressure Vessel Code, Section IX and *it does not*. Rather it presents the results of research on the combined effects of using a single welding process, GMAW, for the root pass and fill passes along with varying the interpass temperature from 100 to 500°F in multipass weldments. Satisfactory and robust weld parameters using GMAW for the open root pass were never discovered but this process does show promise and will be investigated further in the future. The upper limit of interpass temperature for these alloys was not defined in this study. The author is in the process of expanding current laboratory capabilities to undertake this type of research. A study using GTAW for the open root pass as the baseline welding procedure and varying the interpass temperature as was done in this study is planned for the spring of 2012. Mechanical testing and metallurgical analysis of the HAYNES 230 alloy weldments will be started in the fall of 2011.

## **Chapter 6 Recommendations for Future Research**

The follow areas are recommended for further research:

1. Complete the mechanical testing, tensile, bend, and hardness tests, for HAYNES 230 alloy
2. Complete the metallurgical examination for HAYNES 230 alloy
3. Develop welding wave forms specific to these nickel based alloys and a welding procedure specification for these alloys.
4. Use the GTAW process for the open root pass for a baseline comparison to this study.
5. Develop GMAW root pass parameters that are less sensitive to process variations and that are more robust.
6. Determine the upper limit for interpass temperature for these alloys.

## References

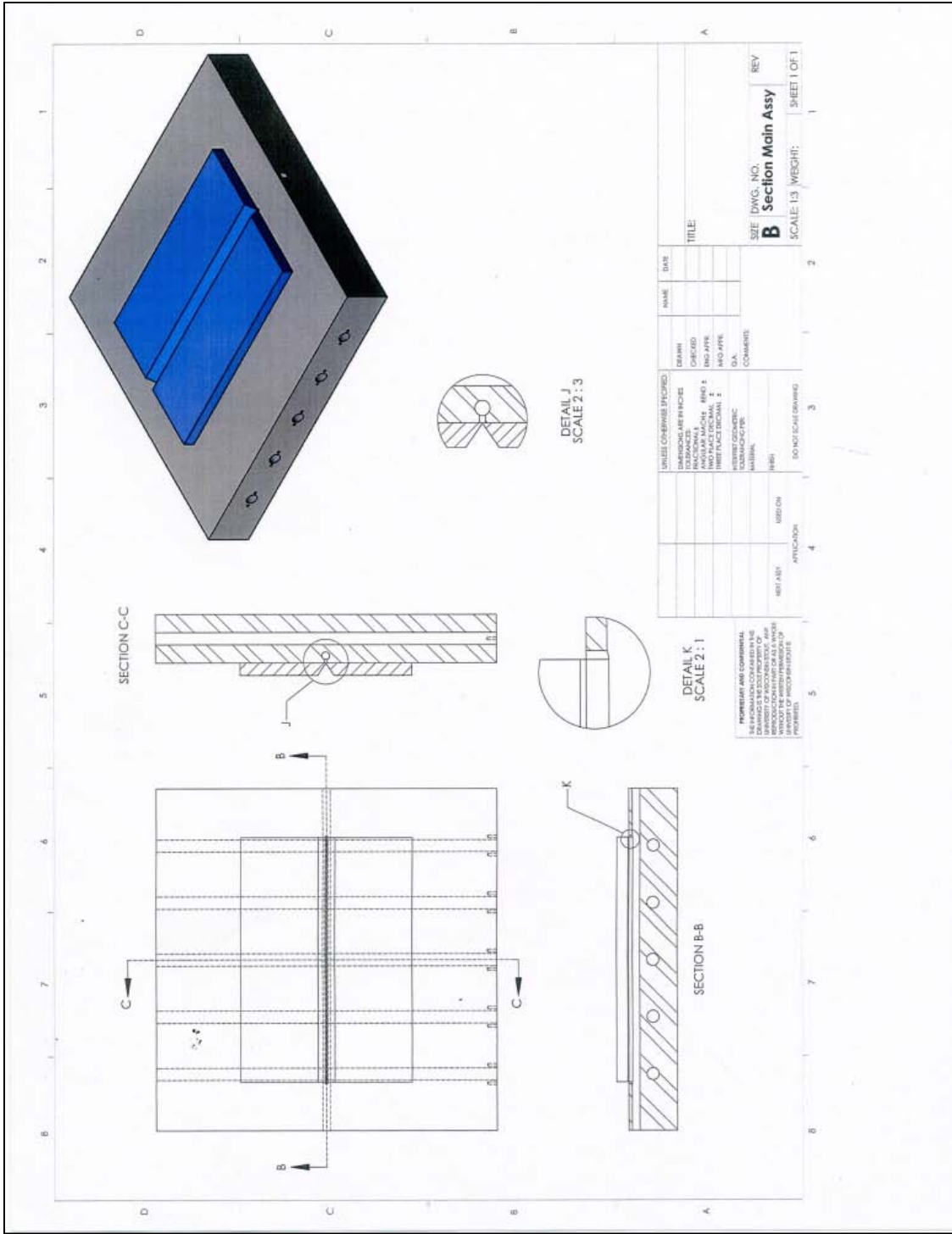
1. Mankins, W., L. and Lamb, S., *Nickel and Nickel Alloys*. in Properties and Selection: Nonferrous Alloys and Special Purpose Materials, Vol. 2, Metals Handbook, 10<sup>th</sup> ed., ASM International, 1990, pp 428-445.
2. Askeland, Donald, L., *The Science and Engineering of Materials*. 5<sup>th</sup> edition, Thomson Canada Limited, 2006, pp 516-519.
3. Mangonon, Pat, L., *The Principles of Material Selection for Engineering Design*. Prentice Hall, NJ, 1999, pp 592-600.
4. Rebak, Raul, B., *Selection of Corrosion Resistant Materials for Nuclear Waste Repositories*. UCRL-PROC-221893, Materials and Science Technology, Cincinnati, OH, 2006.
5. Dawson, Jim, *As Decision Time Approaches for Radioactive Waste Repository, a Mountain of Issues Still Unresolved*. Physics Today, Vol. 54, issue 11, p23, 2001
6. Davis, J., R., *Corrosion of Weldments*. Chapter 7, Corrosion of High-Nickel Alloy Weldments, ASM International, Materials Park, OH, 2006, pp 125-142.
7. Viswanathan, R., *Materials for Ultrasupercritical Coal-Fired Power Plant Boilers*. VTT Symposium, Vol. 233, pp 97-113, 2004.
8. Mohn, Walter, R., *Considerations in Fabricating USC Boiler Components from Advanced High Temperature Materials*. Advances in Materials Technology for Fossil Power Plants; Proceedings from the Fourth International Conference, October 25-28, 2004, Hilton Head Island, SC pp165-176, 2005.
9. Borden, M., P., *Weldability of Materials for Ultrasupercritical Boiler Applications*. Advances in Materials Technology for Fossil Power Plants; Proceedings from the Fourth International Conference, October 25-28, 2004, Hilton Head Island, SC p837-853, 2005.
10. Pike, L.,M., *Haynes 282<sup>TM</sup> Alloy-A New Wrought Superalloy Designed for Improved Creep Strength and Fabricability*. Proceedings of the ASME Turbo Expo 2006; presented at the 2006 ASME Turbo Expo; May 6-11, 2006 Barcelona Spain, vol 4, pp1031-1039, ASME, New York, NY, 2006.
11. Klarstrom, Dwaine, L., *Rejuvenation Heat Treatment and Weld Repairability Studies of Haynes 230 Alloy*. International Gas, Turbine, and Aerospace Congress, Munich, Germany, May 8-11, 2000, Paper 2000-GT-629.

12. Section VIII, Pressure Vessels, Division 1, ASME Boiler and Pressure Vessel Code, 2007, ASME International, New York, NY.
13. Welding Handbook, 9<sup>th</sup> edition, Volume 1: Welding Science and Technology, American Welding Society, Miami, FL, 2001, pp130-140.
14. Cieslak, Michael, J., *Cracking Phenomena Associated with Welding*. Vol 6, Welding, Brazing, and Soldering, Metals Handbook, 10<sup>th</sup> ed., ASM International, 1990, pp 88-96.
15. ANSI/AWS A3.0-94, Standard Welding Terms and Definitions, American Welding Society, Miami, FL, 1994.
16. ANSI/AWS D1.1-96 Subsection 3.5, Minimum Preheat and Interpass Temperature Requirements, Structural Welding Code – Steel, American Welding Society, Miami, FL, 1996.
17. Kou, Sindo, *Welding Metallurgy*, 2<sup>nd</sup> ed. Wiley, New York, 2003, pp 55-57.
18. Welding Handbook, 9<sup>th</sup> edition, Volume 1: Welding Science and Technology, American Welding Society, Miami, FL, 2001, pp 544-550.
19. Beres, Lajos, *Determination of an optimized Interpass Temperature for the Welding of Martensitic Steels*, The International Journal for the Joining of Materials, Vol. 9, Issue 1, pp 16-19, 1997.
20. Trevisan, Roseana, E., *Effect of Interpass Temperature on Morphology, Microstructure, and Microhardness of Welded API 5L X65 Steel*, Proceedings of the 4<sup>th</sup> International Pipeline Conference, Vol A, pp 327-331, 2002 IPC2002-27112, Calgary, Alberta, Canada.
21. Lord, Mike, *Interpass Temperature and the Welding of Strong Steels*, *Welding in the World*, Vol. 41, Issue 5, pp 452-459, Pergamon Press Oxford 1998.
22. Lee, C., H., *The Effect of Preheat and Interpass Temperature on Corrosion Behavior of Austenitic Stainless Steel*, AWS Convention, Dallas Texas, pp 197-199, 1984.
23. Reed, R. C., *A Simple Model for Multipass Steel Welds*. *Acta Metall. Mater.* Vol. 42, No. 11, pp. 3663-3678, 1994.
24. Welland, W. G., *Producing Strong Welds in 9% Nickel Steel*. *Welding Journal*, Vol. 57, Issue 9, pp. 263s-271s, 1978.

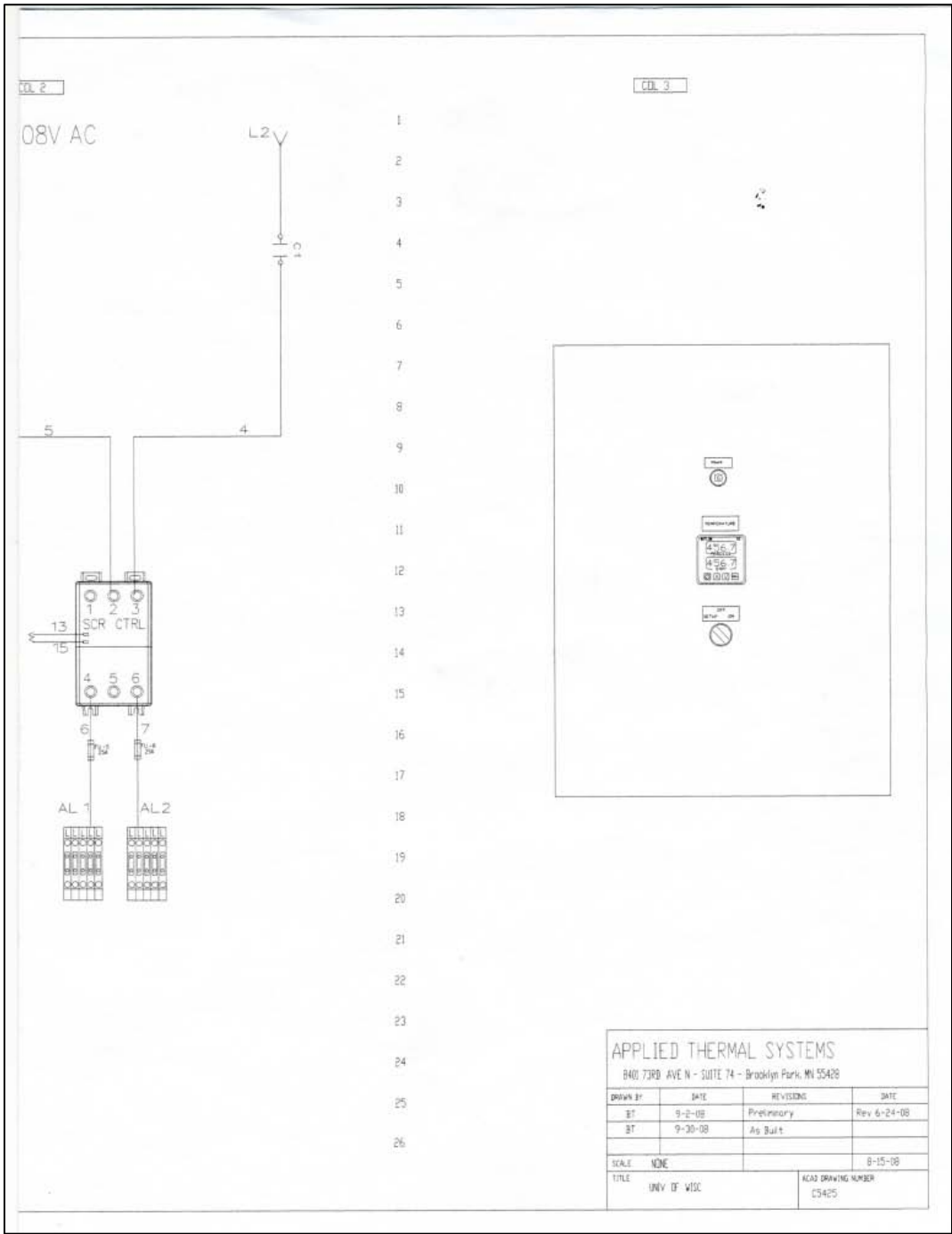
25. Haro, Sergio, *Study of Weldability of a Cr-Si Modified Heat-Resisting Alloy*, Materials Chemistry and Physics, 77 (2002), pp.831-835.
26. Omar, A., A., *Effects of Welding Parameters on Hard Zone Formation at Dissimilar Welds*. Welding Journal, Vol 67., February, 1998, pp. 86s-93s.
27. Ginn, B. J., Gooch, T. G., Davey, T. G., *Effects of interpass Temperature when Welding Austenitic Stainless Steel*. Metal Construction, Vol. 15, issue 12, pp 745-752, 1983.
28. Welding Handbook, 8<sup>th</sup> edition, Volume 3: Materials and Applications, American Welding Society, Miami, FL, 1996, pp 218-288.
29. Tillack, Donald, J., *Selection of Nickel, Nickel-Copper, Nickel-Chromium, and Nickel-Chromium-Iron Alloys*. in Welding, Brazing, and Soldering, Vol. 6, Metals Handbook, 10<sup>th</sup> ed., ASM International, 1990, pp 88-96.
30. Rowe, M. D., *Weldability of a Corrosion-Resistant Ni-Cr-Mo-Cu Alloy*. Welding Journal, November, 2003 pp313s-320s.
31. Ernst, S. C.; *Weldability Studies of Haynes 230 Alloy*. Welding Journal, Vol. 73, no. 4, April 1994, pp 80s-89s.
32. Avery, Richard E. and Tuthill, Authur, H., *Guidelines for the Welded Fabrication of Nickel Alloys for Corrosion-Resistant Service*. A Nickel Development Institute Reference Book, 1994.
33. Rowe, M., D., Manning, P., E., *Welding of Nickel-Base Alloys*. International Institute of Welding (Asian Pacific International Congress), 2002, Paper 11.
34. Rowe, M., D., Ishwar, V., R., Klarstrom, D., L., *Properties, Weldability, and Applications of Modern Wrought Heat-Resistant Alloys for Aerospace and Power Generation Industries*. Journal of Engineering for Gas Turbines and Power, April, 2006, Vol. 128, pp 354-361.
35. Klarstrom, D., L., *The Development of Haynes 230 Alloy*. Materials Design Approaches and Experiences, 2001, pp 297-307, Mineral, Metals, and Materials Society
36. Matthews, S., J., *Simulated Heat-Affected Zone Studies of Hastelloy Alloy B-2*. Welding Journal, March, 1979, pp 91s-95s.
37. HASTELLOY® C-2000® Alloy, Alloy Data Sheet H-2118, Haynes International, Inc., Kokomo, IN, 2005.

38. HASTELLOY® B-3® Alloy, Alloy Data Sheet H-2104A, Haynes International, Inc., Kokomo, IN, 1995.
39. HAYNES® 230® Alloy, Alloy Data Sheet H-3000H, Haynes International, Inc., Kokomo, IN, 2004.
40. Cuhel, Jim, *GMAW Options Offer Increased Productivity for Pipe Fab Shops*, Welding Journal, June, 2008, pp 66-68.
41. AWS B4.0:2007, *Standard Methods for Mechanical Testing of Welds*, American Welding Society, Miami, FL.
42. ASTM E8-04, Standard Test Method for Tension Testing of Metallic Materials, ASTM International, West Conshohocken, PA.
43. ASTM G 28 -02, *Standard Test Methods of Detecting Susceptibility to Intergranular Corrosion in Wrought, Nickel-Rich, Chromium-Bearing Alloys*, ASTM International, West Conshohocken, PA.
44. Dupont, John, N, Lippold, John, C., and Kiser, Samuel, D., *Welding Metallurgy and Weldability of Nickel Based Alloys*, John Wiley and Sons, Hoboken, NJ, 2009.
45. Section IX, Qualification Standard for Welding and Brazing Procedures, Welders, Brazers, and Welding and Brazing Operators, ASME Boiler and Pressure Vessel Code, 2007, ASME International, New York, NY.
46. Phull, Bopinder, *Evaluating Intergranular Corrosion*, ASM Handbook, Volume13A, Corrosion: Fundamentals, Testing, and Protection, ASM International, Materials Park, OH, 2003, pp 568-571.
47. Klarstrom, D., L., *A New Ni-Mo Alloy with Improved Thermal Stability*, Pro. 12<sup>th</sup> Intl. Corrosion Congress, September, 1993, Houston, TX, NACE International, 1993.
48. *Corrosion of Nonferrous Alloy Weldments*, ASM Handbook, Volume13A, Corrosion: Fundamentals, Testing, and Protection, ASM International, Materials Park, OH, 2003, p 317.
49. Welding Handbook, 9<sup>th</sup> edition, Volume 2: Welding Processes, American Welding Society, Miami, FL, 2004.
50. Welding Handbook, 9<sup>th</sup> edition, Volume 1: Welding Science and Technology, American Welding Society, Miami, FL, 2001.

## **Appendix A Heating Fixture Drawing**



## **Appendix B Temperature Controller Electrical Schematic**



APPLIED THERMAL SYSTEMS  
 8400 73RD AVE N - SUITE 74 - Brooklyn Park, MN 55428

DRAWN BY	DATE	REVISIONS	DATE
BT	9-2-08	Preliminary	Rev 6-24-08
BT	9-30-08	As Built	
SCALE NONE			8-15-08
TITLE UNV OF WISC		KCAD DRAWING NUMBER CS425	

